AD-A075 265 GEORGIA INST OF TECH ATLANTA ENGINEERING EXPERIMENT --ETC F/G 17/5
INVESTIGATION OF MILLIMETER WAVE AND FAR INFRARED MULTIWAVELENG--ETC(U)
SEP 79 R G SHACKELFORD, J J GALLAGHER DAAG29-77-C-0026
UNCLASSIFIED GIT/EES-A-1985 ARO-15277.2-A-P NL

1 OF 1
AD A 075265

END
DATE FILMED
11 -79
DDC

LEVEL II

INVESTIGATION OF MILLIMETER WAVE AND FAR INFRARED MULTIWAVELENGTH SYSTEMS

FINAL REPORT
A-1985

R. G. Shackelford, J. J. Gallagher, R. W. McMillan
G. R. Loefer, W. M. Penn, W. A. Holm and W. S. Foster

September 17, 1979

U. S. ARMY RESEARCH OFFICE

Contract No. DAAG29-77-C-0026

GEORGIA INSTITUTE OF TECHNOLOGY
ENGINEERING EXPERIMENT STATION
ATLANTA, GEORGIA 30332

(6) INVESTIGATION OF MILLIMETER WAVE AND FAR INFRARED MULTIWAVELENGTH SYSTEMS.

(9) FINAL REPORT. 1 Jul 77-31 Mar 79
A-1985

(14) GIT/EES-A-1985

(10) R. G./Shackelford, J. J./Gallagher, R. W./McMillan, G. R./Loefer, W. M./Penn, W. A. Holm and W. S. Foster

(11) 17 September 1979

(12) 68

U. S. ARMY RESEARCH OFFICE

(15) Contract No. DAAG29-77-C-0026

(18) ARO

GEORGIA INSTITUTE OF TECHNOLOGY
ENGINEERING EXPERIMENT STATION
ATLANTA, GEORGIA 30332

(19) 15277.2-A-P

APPROVED FOR PUBLIC RELEASE:
DISTRIBUTION UNLIMITED

153 850

THE FINDINGS IN THIS REPORT ARE NOT TO BE CONSTRUED AS AN OFFICIAL DEPARTMENT OF THE ARMY POSITION, UNLESS SO DESIGNATED BY OTHER AUTHORIZED DOCUMENTS

SECURITY CLASSIFICATION OF THIS PAGE (When Data Entered)

REPORT DOCUMENTATION PAGE

READ INSTRUCTIONS BEFORE COMPLETING FORM

1. REPORT NUMBER: ~~A-1985~~
2. GOVT ACCESSION NO.
3. RECIPIENT'S CATALOG NUMBER

4. TITLE (and Subtitle): Investigation of Millimeter Wave and Far Infrared Multiwavelength Systems
5. TYPE OF REPORT & PERIOD COVERED: Final Report 7/01/77 to 3/31/79
6. PERFORMING ORG. REPORT NUMBER: A-1985

7. AUTHOR(s): R. G. Shackelford, J. J. Gallagher, R. W. McMillan, G. R. Loefer, W. M. Penn, W. A. Holm and W. S. Foster
8. CONTRACT OR GRANT NUMBER(s): DAAG29-77-C-0026

9. PERFORMING ORGANIZATION NAME AND ADDRESS: Georgia Institute of Technology, Engineering Experiment Station, Atlanta, Georgia 30332
10. PROGRAM ELEMENT, PROJECT, TASK AREA & WORK UNIT NUMBERS

11. CONTROLLING OFFICE NAME AND ADDRESS: U. S. Army Research Office, P. O. Box 12211, Research Triangle Park, NC 27709
12. REPORT DATE: 17 September 1979
13. NUMBER OF PAGES

14. MONITORING AGENCY NAME & ADDRESS(if different from Controlling Office)
15. SECURITY CLASS. (of this report): Unclassified
15a. DECLASSIFICATION/DOWNGRADING SCHEDULE

16. DISTRIBUTION STATEMENT (of this Report)

Approved for public release; distribution unlimited.

17. DISTRIBUTION STATEMENT (of the abstract entered in Block 20, if different from Report)

18. SUPPLEMENTARY NOTES

The view, opinions, and/or findings contained in this report are those of the author(s) and should not be construed as an official Department of the Army position, policy, or decision, unless so designated by other documentation.

19. KEY WORDS (Continue on reverse side if necessary and identify by block number)

Laser/Millimeter Wave Hybrid System
Atmospheric Attenuation
Near Millimeter Wave Systems Applications

20. ABSTRACT (Continue on reverse side if necessary and identify by block number)

This report summarizes the results of three related tasks performed under the subject contract: Hybrid Millimeter Wave/CO_2 Laser Target Acquisition System; Millimeter Wave Propagation Through Battlefield Dust; and Report of NMMW System Subpanel. A full final report has been published on each subtask, and is available through the cognizant Army Organizations.

DD FORM 1 JAN 73 1473 EDITION OF 1 NOV 65 IS OBSOLETE

Unclassified

SECURITY CLASSIFICATION OF THIS PAGE (When Data Entered)

TABLE OF CONTENTS

I. INTRODUCTION

II. SUMMARY OF WORK

A. Volume I - "Hybrid Millimeter Wave CO_2 Laser Target Acquisition System" 1

B. Volume II - "Millimeter Wave Propagation Through Battlefield Dust" 11

C. Volume III - "Report on NMMW System Subpanel" 18

Appendix I - Paper Presented To: The 6th Annual Tri-Services Submillimeter Wave Conference 19

Appendix II - Paper Presented To: Workshop on Millimeter and Submillimeter Atmospheric Propagation Applicable to Radar and Missile Systems 28

Appendix III - Paper Presented To: 23rd Annual SPIE International Technical Symposium 38

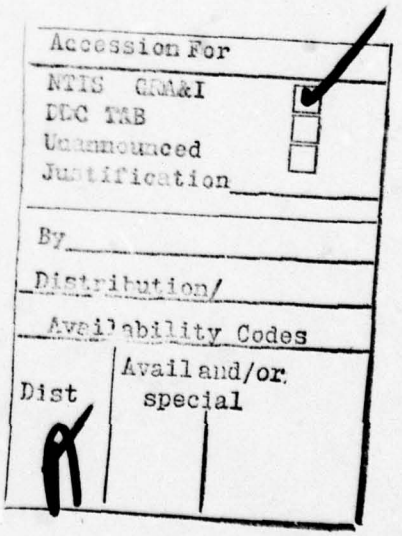

LIST OF FIGURES

1. Block Diagram of the Common Aperture CO_2 Heterodyne Targeting System 3

2. Block Diagram of the CO_2 Laser Targeting System Reconfigured for FM/CW Operation 4

3. Component Layout of the CO_2 Heterodyne System 5

LIST OF TABLES

1. Summary of Results of Millimeter Wave Propagation Through Explosions 14

I. INTRODUCTION

A research program entitled "Investigation of Millimeter Wave and Far Infrared Multiwavelength Systems" was performed under Contract No. DAAG29-77-C-0026. This program encompassed three tasks, each of which was performed under the cognizance and direction of different Army Commands. The final report has been prepared in three volumes partitioning the results of work on the individual tasks into more useable documents for those interested in only one of these efforts. The report is organized as follows:

Volume		Cognizant Organization
I.	Hybrid Millimeter Wave/CO_2 Laser Target Acquisition System	U. S. Army ERADCOM Ft. Monmouth, N. J.
II.	Millimeter Wave Propagation Through Battlefield Dust	Atmospheric Sciences Laboratory White Sands Missile Range, N. M.
III.	Report of NMMW System Subpanel	Harry Diamond Laboratories Adelphi, MD

This report is comprised of a summary of the work performed under the individual tasks listed above, and three papers which reported the significant results of this work. The interested reader is referred to the cognizant Army organizations for a full technical report on each of the tasks included in this program effort. The internal Georgia Tech project number is A-1985.

II. SUMMARY OF WORK

A. Volume I - "Hybrid Millimeter Wave CO_2 Laser Target Acquisition System"

Tactical surveillance and weapon guidance systems depend critically on the ability to acquire, identify and precisely locate targets of military significance. The conventional microwave radars which have traditionally been used for target acquisition by the Army can rapidly search large volumes of space and locate potential targets. However, these systems generally lack the resolution to identify targets and locate them with the accuracy required for weapon delivery. Electro-optical systems operating in the visible and infrared can quite easily achieve this resolution but at the cost of narrower fields-of-view. A narrow field-of-view greatly increases search times over a given volume. Thus, the concept was formed of an electro-optical/microwave radar synergism in which the radar, from a rapid, large volume search, provides low resolution target coordinates around which the E-O system does a high resolution, low volume scan to produce accurate target coordinates and target identification.

As initially conceived, this program was to include two phases: Phase I involved the investigation of radar parameters affecting the required field-of-view of the E-O sensor, and a demonstration of handover from a 70 GHz surveillance radar to an E-O sensor system simulated by a TV sensor equipped with a zoom telephoto lens; Phase II was to involve a demonstration of handover and pointing refinement by a hybrid system consisting of a 70 GHz radar and an active CO_2 laser scanning sensor system coupled electrically through the radar display and cursors.

The first phase of this program was successfully demonstrated in a series of tests which were reported in a paper given at the DARPA Sixth Annual Tri-Services Submillimeter Wave Conference, and included herein as Appendix I. The important result of these tests was that targets could be located with the radar by an operator-positioned cursor to within a standard deviation of 0.5 - 1.0 mrad even though the radar beamwidth was 9.6 mrad. In view of these results, the E-O system design was based on the assumption that the target line-of-sight (LOS) could be reliably determined to within $\pm$ 1 mrad in both elevation and azimuth. Tests

employing a TV sensor with zoom telephoto lens mechanically boresighted to the radar confirmed that a 3 mrad field-of-view was adequate to insure that the target would always be located in the E-O sensor's FOV at the instant of handover. Handover from the cursor control to a two-axis gimbal positioner for the E-O system was demonstrated, but slow drifts in pointing direction prevented full utilization of E-O system resolution. In summary, these facts indicate that LOS pointing accuracy can, by a combination of radar beam splitting and handover to an E-O sensor system, be improved to the resolution limit of the E-O sensor platform (~0.1 mrad). Thus, the improvement in terms of the radar beamwidth (~10 mrad) would be 100:1.

During the second phase of this program, the funding resources were exhausted in the development of the CO_2 sensor system and modifications to the control circuitry and mechanical configuration of the two-axis gimbal, which was furnished GFE, before any data on handover and pointing accuracy could be obtained. The development of the CO_2 sensor system was cost-shared in that all components were purchased by Georgia Tech, and approximately three man-months were expended by EES personnel in its development without cost to the U. S. Army. The system optical design was to be compatible with a pulsed CO_2 laser under development by ERADCOM, but unfortunately this device was not available during the course of the program. In its place, a CW laser was employed, and internal reflections within the optical system resulted in the necessity of a design modification to allow system operation in the FM/CW mode. Block diagrams of the common aperture CO_2 laser targeting system are shown as configured for CW/heterodyne operation in Figure 1 and CW/FM operation in Figure 2. The component layout of this system is shown in Figure 3.

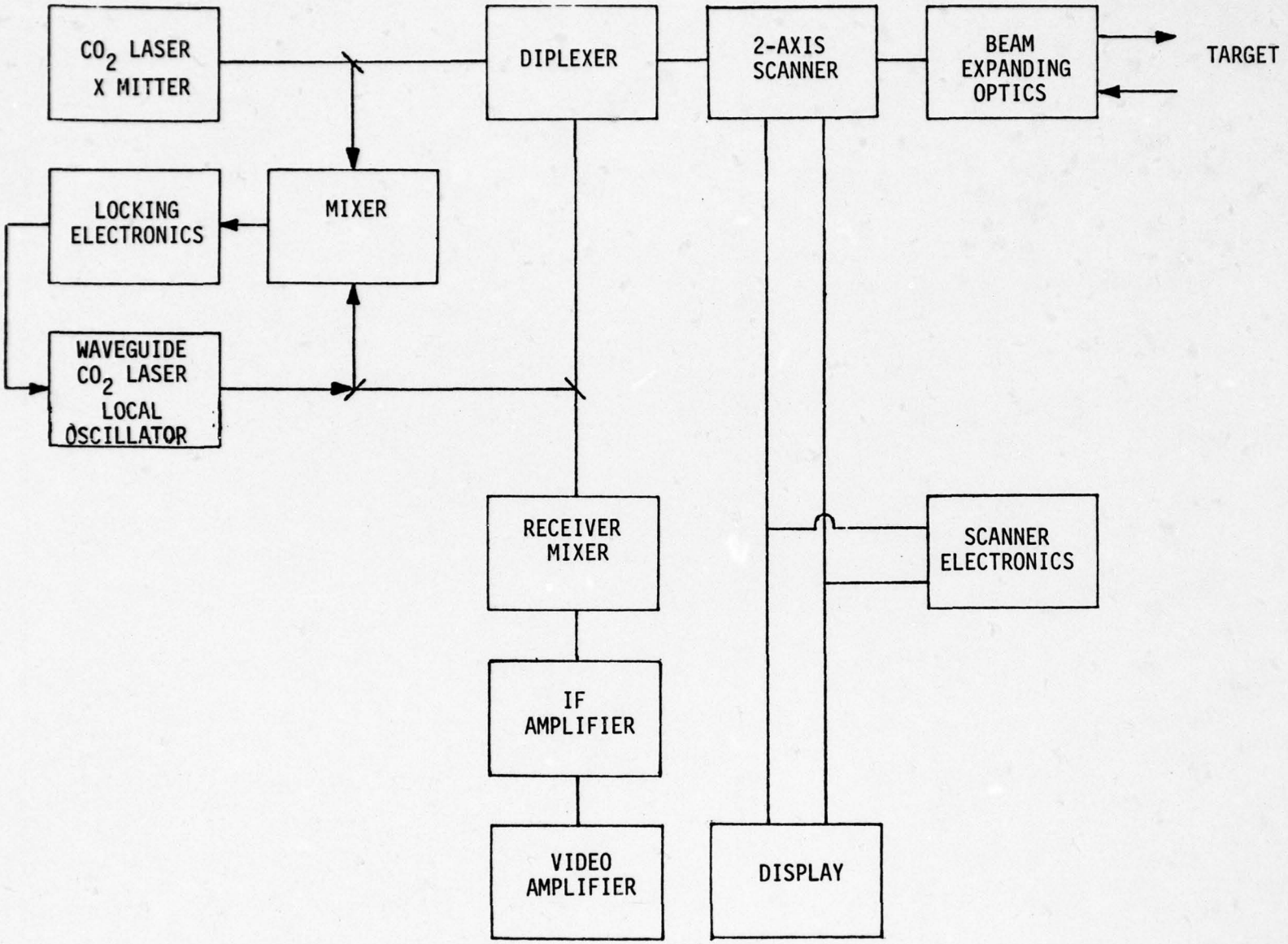

Figure 1. Block Diagram of the Common Aperture CO_2 Heterodyne Targeting System

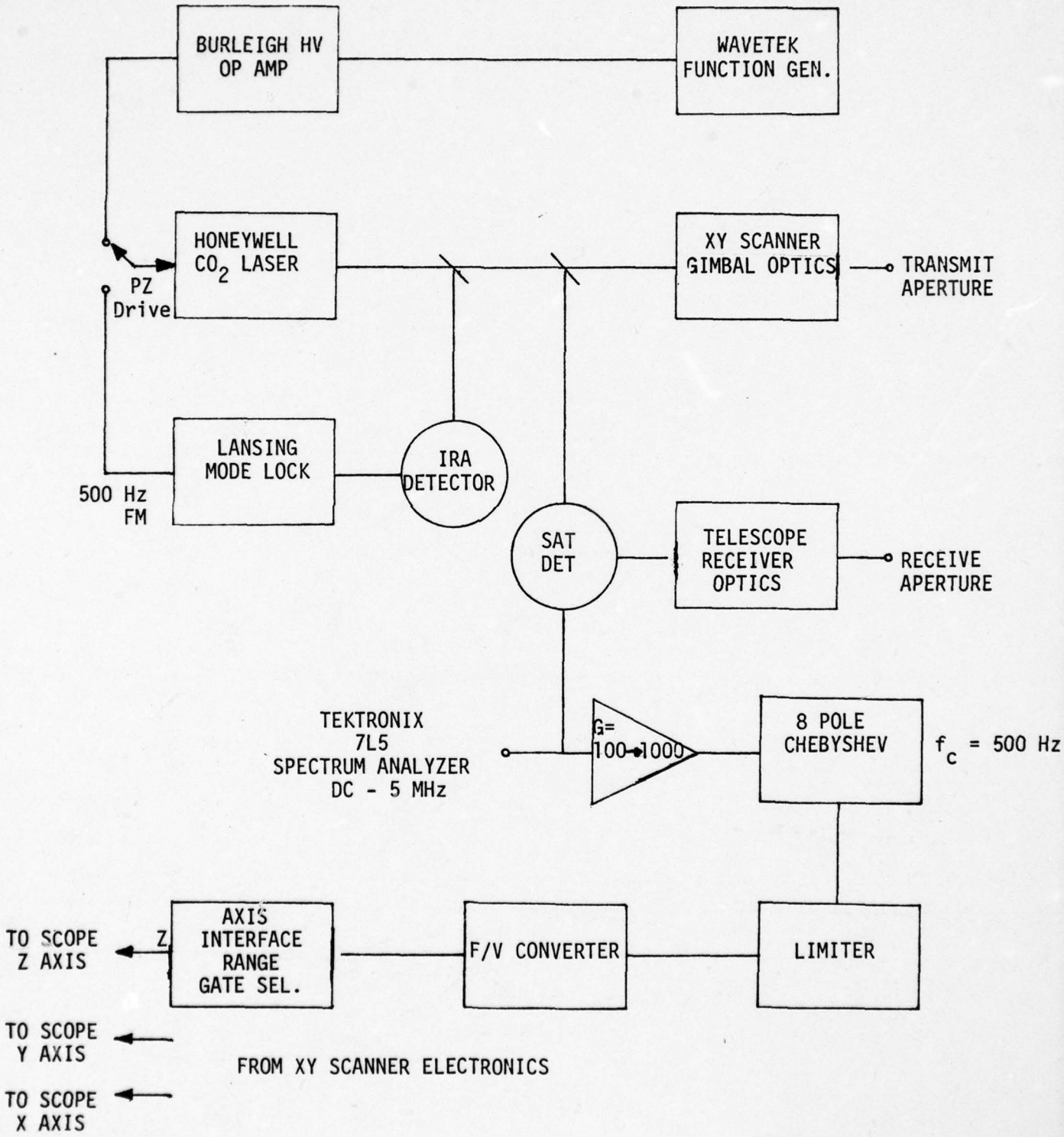

Figure 2. Block Diagram of the CO_2 Laser Targeting System Reconfigured for FM/CW Operation

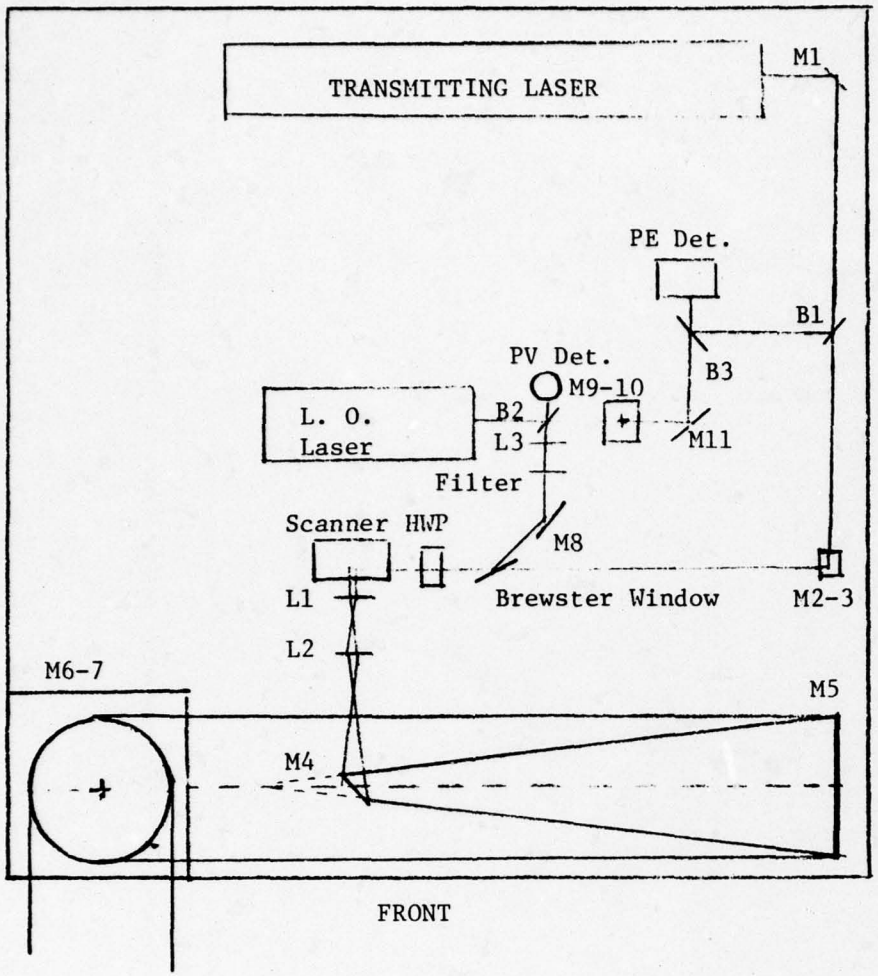

Figure 3. Component Layout of the CO_2 Heterodyne System

During this program, it was demonstrated that a combination of E-O and millimeter wave sensors can be effectively employed to improve the accuracy of line-of-sight pointing and provide a means for target identification in conditions of high visibility. These tests were performed with a 70 GHz rapid scanning millimeter radar and a TV sensor with handover initiated by the radar azimuth-elevation display cursors. Tests were performed with the TV system mechanically boresighted through the millimeter scanner's optical periscope, and with the E-O field-of-view coupled to the radar through the radar cursor E-O/gimbal electronic interface.

The final goal of the program was to demonstrate handover from the millimeter radar to a CO_2 laser targeting system which was under development by Georgia Tech for this program. This goal was not achieved because of problems encountered with operation of the CO_2 system in a common aperture configuration with a CW laser transmitter.

A pulsed CO_2 laser under development by ERADCOM would have met the technical requirements for this application, but unfortunately was not available during this program's performance period. At the beginning of the system development effort, no other pulsed CO_2 laser was found with the required combination of pulse energy and pulse repetition frequency, and hence the only alternative available was to convert the system to FM/CW operation to separate the target return from internal backscatter in the frequency domain. This conversion was not successful because of amplitude modulation noise generated by nonlinear response of the PZ mode controller of the CW laser when driven to achieve the required FM modulation.

The modifications required to the CO_2 system and a test plan for achieving the program goals are discussed in the following sections. In view of the positive results obtained during the millimeter radar/TV system tests, it is strongly urged that this program effort be continued, and that the performance of a hybrid configuration employing both an active millimeter sensor and an active CO_2 laser sensor be implemented and evaluated.

In order to achieve the goals for evaluation of system performance and optimization of the hybrid concept in terms of operating mode, spectral assignment and radiation characteristics, further work will be required. Based on this program, three general areas for emphasis have been defined: 1) hardware improvements to the present system, 2) extended field tests with a modified system configuration, and 3) studies to define concepts and techniques for improving performance of hybrid systems for target engagement.

1. System Improvements

The primary requirement for improvement of the CO_2 system's performance is the acquisition of a pulsed laser with the appropriate pulse energy and prf. Based on the calculations presented in Section II-A, the minimum energy per pulse should be about 100 mJ for a system capable of operation over moderate conditions of inclement weather (light rain or fog) and the prf should be about 20 kHz for flicker-free display of a 32 x 32 point image. The required pulse energy could be reduced significantly for operation only under high visibility conditions (0.01 mJ would be adequate), and the prf could be reduced by signal processing. The minimum prf for an operational system, however, would be about 15 kHz for a 10 mph target at 1 km (0.3 mrad uncertainty in target centroid for a 3 mrad FOV). It is anticipated that these pulsed CO_2 laser requirements can be met within the current state-of-the art.

The current CO_2 system has been designed to provide optimum performance within the economic constraints of the program; however, the limitations due to inadequate performance of some of the key components were documented during the program. Perhaps the most serious limitation on system performance is the gimbal mount which is marginally stable with the weight of the pointing reflector. Other areas in which system performance can be improved are by the acquisition of detectors with better sensitivity and larger bandwidth, upgrading of the electronics processing system, and the acquisition of a display system with storage

capability. Of less immediate concern, but of eventual importance for remote field operations would be improved system packaging including a compressed optical train and smaller lasers, a sealed cover with infrared windows for operation in inclement weather, and a general mechanical hardening of the system to withstand shock and vibration resulting from operation of the van over rough terrain.

The 70 GHz radar system being used as the acquisition radar does not represent a potential tactical radar. Further, to effect improved performance, it is highly desirable that the 70 GHz radar be replaced by a 95 GHz radar. The cost of developing a new radar, however, would be high (on the order of $300K). A number of potential ways of obtaining a 95 GHz radar without incurring the high cost of a new radar development program are suggested. The lowest cost option is to use the existing radar but even this option would require a new magnetron and some work to refurbish the radar.

The most desirable test configuration would be based on the use of a tactical radar. The Georgia Institute of Technology is currently pursuing the design and fabrication of a dual frequency tracking radar for the General Electric AVADS systems. This system won't be ready for field tests for about a year. An expression of interest by the Army could , however, possibly speed up the development. If it were desired to pursue this approach, Georgia Tech would discuss the utilization of the radar with General Electric.

A second alternative is to use the transmitter from one of the Georgia Tech 95 GHz radars in conjunction with a 95 GHz monopulse antenna owned by Georgia Tech. A monopulse receiver would have to be built. A modified HAWK pedestal would be used to scan the antenna. This would not provide a tactical radar configuration, but it would provide the essential elements of a simulated tactical radar.

The final alternative is to build a 95 GHz version of the geodesic lens antenna, and integrate it with one of the 95 GHz instrumentation radars owned by Georgia Tech. Rather than mount the radar in the

existing van, it would be mounted in another van provided by Georgia Tech or one supplied by the Army. This technical approach represents a low technical risk and does not require modifications to the instrumentation radar.

The recommended approach is to build a three channel monopulse receiver which can be used with Georgia Tech 95 GHz transmitter and antenna. This approach is preferred since it is the closest to a tactical radar configuration and it requires the least fabrication of new hardware. It should also require the shortest amount of development time.

For the extended tests, the minimum recommended system improvements would include acquisition of a pulsed CO_2 laser transmitter, upgrading the IR detectors and processing electronics and the acquisition of a new millimeter magnetron. The other suggested improvements could be brought along as a part of a longer range program to coincide with the comparison tests between this system and other candidate systems.

2. Extended Field Tests

Extended (2-3 months) field tests should be performed with the hybrid system to evaluate its potential for improved performance under simulated tactical conditions.

It is recommended that these tests be performed at a remote site reasonably close to Atlanta, such as Ft. Benning, Georgia, in order to achieve greater flexibility in target availability and range topography. The extended field tests would be similar to those performed under the current contract but would be much more extensive in terms of the data collection and analysis. Also, improvements suggested by the earlier field tests would be further investigated and incorporated within the scope and limitations of the funding. Thirdly, if the tests are held at the Ft. Benning site, a wider variety of targets, target ranges and target orientations would be available.

The objective of the field tests would be to produce a ten to fifteen minute video tape demonstrating the system performance against tactical ground targets such as armored vehicles. The video tape would document approximately 100 measurements which would be obtained on two targets at four different ranges for four aspect angles and three polarization conditions. Environmental conditions would be monitored and recorded for each test. These parameters would include wind speed, relative humidity and temperature, and also particle size distribution and an estimate of optical visibility. The final report would fully document the field tests, and also include conceptual drawings of potential field-ready versions of the system.

3. Studies

As an important adjunct to the field tests, several studies should be initiated to identify and refine concepts and techniques for hybrid system evolution. These studies would include an assessment of innovative component designs, improved interface techniques, system hardware integration for multifunctional use, and optimum operating modes. Some suggested topics for this study are listed below:

A. Common Aperture Laser/Radar System
B. 94 GHz Coherent Radar for Hybrid System
C. Pulsed Heterodyne CO_2 Subsystem
D. Design of Small, Sealed TEA Laser
E. Tracking and/or Designation With CO_2 Laser
F. Target Identification/Recognition With CO_2 Laser

B. Volume II - "Millimeter Wave Propagation Through Battlefield Dust"

As the state of millimeter wave technology improves, this wavelength region is becoming increasingly attractive to military systems designers. Microwave systems using millimeter waves have the advantage of improved resolution with smaller antennas, and the availability of reliable solid state sources has provided the means to build small, lightweight systems which have low power consumption.

A potentially severe problem in the use of millimeter waves in battlefield situations is the possible degradation of these systems caused by atmospheric propagation effects. Some fairly extensive studies and measurement programs have led to some understanding of the performance of millimeter systems in rain and fog, although much work remains to be done in this area, but little work has been done to characterize millimeter propagation through battlefield dust. This report gives the results of a series of experiments conducted at White Sands Missile Range by personnel of the Georgia Tech Engineering Experiment Station in late September and early October 1978 which attempt to fill this gap in knowledge about millimeter wave propagation. These measurements were part of the DIRT I program conducted by the Atmospheric Sciences Laboratory. A paper summarizing the results of this work was submitted to the workshop on millimeter and submillimeter atmospheric propagation held in March, 1979 at Redstone Arsenal, Alabama, and included herein as Appendix II.

During most of the experiments, simultaneous measurements were made at 94 and 140 GHz; however a power supply failure caused the 140 GHz receiver to be inoperative, so that only 94 GHz measurements were obtained during much of the test.

The simulated battlefield dust was generated by detonating TNT charges, static detonation of 155 mm howitzer projectiles, and live firings of 155 mm howitzers. In addition, a test was conducted on the final day which measured signal degradation caused by simulated battlefield smoke. The aerosols generated during these tests were characterized by a helicopter-borne sensor package.

This report describes the results of propagation tests of millimeter waves through the battlefield aerosols discussed above. Detailed descriptions of the TNT and howitzer projectile firing geometry and the aerosol sensing techniques may be found in the test plan entitled "ASL Battlefield Dust Tests", dated 25 July 1978. For the sake of completeness, brief descriptions of these parameters are given in this report.

The DIRT I objectives are given in the above mentioned test plan and are directed toward providing specific optical data for atmospheric modeling and testing of sampling technology for measuring the optical and physical properties of explosion debris clouds. The E-O apparatus involved in the tests has been described in the test plan and in other reports of the tests. The simultaneous measurements by E-O and millimeter wave systems provide the opportunity for comparison of the effects in the two spectral regions.

DIRT I has provided the first opportunity for observing the effects of tactical size explosions on millimeter wave and E-O propagation. In many events, large and often unexpected attenuations were observed. Whereas damage suffered by equipment in transit caused some limitations and eventual failure of the 140 GHz apparatus, significant data were, in general, obtained. Table 1 summarizes the results of the measurements.

Several conclusions can be drawn from the measurements. As indicated, attenuation in most cases was large. The relatively short recovery time of the attenuated signal indicates that the attenuation was caused by the large pieces of soil blown in the air in the early stage of each event. The residual dust remaining in the air after the initial large particles have settled makes no significant contribution to the attenuation. This result is similar to the results obtained at millimeter wavelengths when propagating through dust raised by vehicles. The signal fluctuations in the majority of the events were large, and their origin has not been fully established. As indicated by the monitoring of the source amplitude stability and the receiver noise level when signal is blocked, the fluctuations probably do not receive a major contribution from the instrumentation. Some contribution could originate from atmospheric fluctuations. Quite probably, the majority of these fluctuations result from multipath effects.

The large beamwidths (~2°) resulted in effects from vehicles, personnel, moving bushes, etc. being observable in the receiver system. A more narrow beam antenna system would minimize these effects. The fluctuations which were observed were of sufficient magnitude to obscure small attenuation effects. Frequency stability of the transmitter and local oscillator was sufficient to keep the signal within the amplifier bandwidth and thereby cause no fluctuations.

During the early events, signal absorption strength was probably greater than indicated since long integration times (1.25 seconds) were used. When the time constants were shortened significant signal increases were noted. The large fluctuations influenced the decision to use long time constants in the early observations. In addition, greater dynamic range in the amplifier systems would have given greater signal sensitivity. Additional effects which influenced the observations included level changes after the event, possibly caused by the explosion, signal drift which presented problems on determining baselines (0 dB) and inaccuracy of start of the event. It is observed that the attenuation of the two signals (94 GHz and 140 GHz) started at different times during some events. The time constants of both systems were the same during the tests. Recorder response may have been the cause of this small discrepancy.

The scintillation during the burning of the diesel oil, motor oil and rubber was very large and exceeded the expected effect. The 3 - 5 dB scintillation would be extremely detrimental to the operation of military systems in the millimeter wavelength region.

The signals obtained during the howitzer firings varied significantly for each event. The strength of the absorption depended on the position of the impact relative to the optical path of the system. The spread in absorption for each salvo resulted from the difference in time for the impact of each round. The positive signal response which was observed for some firings resulted when attenuation was not the greatest and probably when the impact area was not directly in the optical path. As a result, scattering of signal into the receiver by the fragments blown in the air could have been the cause of signal increase.

TABLE 1

SUMMARY OF RESULTS OF MILLIMETER WAVE PROPAGATION THROUGH EXPLOSIONS

DATE	EVENT	FREQUENCY (GHz)	MAXIMUM ATTENUATION (dB)	RECOVERY TIME (sec)	TIME CONSTANT (sec)	COMMENTS
10/02/78	A-1	94	-	-	1.25	Fluctuations, Equipment Problems, etc. Prevented Data Taking; Long Time Constant.
	A-2	94	-	-	1.25	Same as A-1.
	A-3	94	-	-	1.25	Same as A-1.
	A-4	94	-	-	1.25	Same as A-1.
10/03/78	B-1	94	-	-		
		140	6.3	10	0.400	Scintillations and Equipment Failure Hindered the 94 GHz Operation.
	B-2	94	-	-	-	Equipment Failure.
		140	-	-	-	
	B-3	94	7.5	15	0.400	Interesting that 140 GHz Recovered Faster than 90 GHz System; High Scintillation.
		140	7.0	5		
	B-4	94	8.1	<5		Well Defined Absorption.
		140	7.5	<5	0.400	
	B-5	94	7.8	12		Secondary Absorption in Both Channels.
		140	9.3	12	0.400	
	B-6	94	8.7	13		Secondary Absorptions Present.
		140	8.9	13	0.400	
	B-7	94	9.8	10	0.400	Recorder Pen Failure on 140 GHz.
		140	~9.3	-		
	B-8	94	10	10		94 GHz Signal Did Not Return to 0 dB Baseline.
		140	13.2	18	0.400	

TABLE 1 (Continued)

SUMMARY OF RESULTS OF MILLIMETER WAVE PROPAGATION THROUGH EXPLOSIONS

DATE	EVENT	FREQUENCY (GHz)	MAXIMUM ATTENUATION (dB)	RECOVERY TIME (sec)	TIME CONSTANT (sec)	COMMENTS
10/05/78	C-1	94	28	25	0	Scintillation Reduced; Integration Removed; Dynamic Range of Amplifier Insufficient to Show Attenuation Accurately > 28 dB
		140	28	25		
10/06/78	D-1	94	~30	7	0.040	Fluctuations ~ 1 dB; Short Time Constant for D-runs.
		140	~30	15		
	D-2	94	>20	11		Poor 140 GHz Results.
		140	>20	>20	0.040	
	D-3	94	13.9	12		
		140	22	19	0.040	
	D-4	94	25	-		Interpretation Difficult Due to Large Fluctuations and Drift.
		140	25	-	0.040	
10/10/78	C-2	94	>35	-	0	Equipment Problems; Estimate on Attenuation for 94 GHz.
		140	-	-		
10/11/78	E-1	94	-	-	0.004	E-Events 94 GHz Only - No Data Because of Equipment Problems and Large Fluctuations; Estimate 35 - 40 dB.
	E-2	94	-	-	0.004	See Comments on E-1.
	E-3	94	35	5	0.004	Strong Attenuation; Both Traces for 94 GHz.
	E-4	94	-	-	0.004	See Comments on E-2.
10/12/78	F-1	94	-	-	0.040	F-Events: Howitzer Firings; Probably Missed Roac
	F-2	94	20	10-12	0.040	3 Groups of Four 155 mm Howitzer Rounds Max Attenuation is for One Round. Probably Directly in Line of Sight.

TABLE 1 (Continued)

SUMMARY OF RESULTS OF MILLIMETER WAVE PROPAGATION THROUGH EXPLOSIONS

DATE	EVENT	FREQUENCY (GHz)	MAXIMUM ATTENUATION (dB)	RECOVERY TIME (sec)	TIME CONSTANT (sec)	COMMENTS
10/12/78	F-3	94	3-4	10-12	0.040	Attenuation Reduced, Possibly Not Directly in Line of Sight; One salvo of This Event Missed Road.
	F-4	94	-	-	0.040	Probably Missed Road.
10/13/78	F-1	94	10, 6	4, 1	0.040	Two Salvos of 4 Rounds Each; Second Salvo Reduced Because of Impact Region.
	F-2	94	6	3-4	0.040	Both Salvos Show Strong Absorption Inversion; Possibly Not Directly in Line of Sight.
	F-3	94	9, 8	4-5	0.040	Strongest Attenuation of Series; Probably Directly in Line of Sight.
	F-4	94	-	-	0.040	Probably Missed Line of Sight.
10/14/78	Test 1	94	19	8	0.040	Tests 1 - 6: Static Firings of Howitzer Rounds at Varying Depths.
	Test 2	94	13	5	0.040	Notice Reduction of Attenuation from Test 1 to Test 6 as Charges are Moved Toward Surface.
	Test 3	94	8.4	4	0.040	See Comments on Test 1 and Test 2.
	Test 4	94	7.8	5	0.040	See Comments on Test 1 and Test 2.
	Test 5	94	6.7	3	0.040	Rounds on Surface.
	Test 6	94	6.1	3	0.040	Rounds on Surface.
	Oil Burn	94	$\sim$1	-	0.040	Total Attenuation Small, but Very Large ($\gtrsim$ 5 dB) Scintillation.

The measurements performed during this program demonstrated the improvements that can be made for future programs. The apparatus employed was mainly laboratory gear with relatively little preparation. The following recommendations will result in improvement in future tests:

The observations should be extended in frequency up to 220 GHz and down to 10 GHz. It is not evident that X-band would not be significantly attenuated by the large masses of material present in the explosion.

Larger ($\approx$ 2 ft.) antennas should be employed to minimize multipath, personnel and vehicle interference, etc. This should lessen the fluctuations observed during most of the firings.

Precision attenuators should be used at all frequencies. They are commercially available up to 140 GHz. No such attenuator was available at the time of these tests.

The systems should be run with short time constants ($\lesssim$ 40 msec.) as it is assumed that the long time constant employed in the early runs resulted in a loss of signal attenuation.

Amplifiers with greater dynamic range than available for these tests should be employed. The amplifiers which were used had greater bandwidth than required. A more narrow bandwidth system would provide an improved signal-to-noise ratio.

For the performance of the measurements, more time prior to each event should be allowed for calibration and review of the previous event. The time between events in DIRT I was limited by the flight of the airborne probe and such limitations on time may exist in future tests. However, sufficient calibration time should be allowed with no personnel or vehicles in the observation path.

C. Volume III - "Report on NMMW System Subpanel"

The third phase of this program required editing and revising of written contributions from panel members to the Harry Diamond Laboratory Near Millimeter Wave Technology Base Study, Volume 3, Systems Applications, which was sponsored by DARCOM and DARPA. A review of the initial submissions by HDL personnel revealed that differences in writing style and technical content could not be resolved by editing as was orginally proposed. As a result, an extensive re-writing of the draft report was necessary. The attached invited paper, presented at the 23rd Annual SPIE International Technical Symposium (August 29, 1979) and the 27th Annual IRIS Symposium (May, 1979) lists the topics of the report and briefly discusses some of the work performed.

A complete copy of the revised report has been submitted to the Harry Diamond Laboratories, and a copy will also be available through the Army Research Office.

C. Volume III - "Report on NMMW System Subpanel"

The third phase of this program required editing and revising of written contributions from panel members to the Harry Diamond Laboratory Near Millimeter Wave Technology Base Study, Volume 3, Systems Applications, which was sponsored by DARCOM and DARPA. A review of the initial submissions by HDL personnel revealed that differences in writing style and technical content could not be resolved by editing as was orginally proposed. As a result, an extensive re-writing of the draft report was necessary. The attached invited paper, presented at the 23rd Annual SPIE International Technical Symposium (August 29, 1979) and the 27th Annual IRIS Symposium (May, 1979) lists the topics of the report and briefly discusses some of the work performed.

A complete copy of the revised report has been submitted to the Harry Diamond Laboratories, and a copy will also be available through the Army Research Office.

APPENDIX I

Paper Presented To:
the 6th Annual Tri-Services
Submillimeter Wave Conference

"Combined Electro-Optical/Millimeter
Wave Radar Sensor System"

PRESENTED TO

DARPA SIXTH ANNUAL TRI-SERVICES
SUBMILLIMETER WAVE CONFERENCE
Washington, D. C. November, 1977

APPENDIX I

COMBINED ELECTRO-OPTICAL/MILLIMETER WAVE RADAR SENSOR SYSTEM

W. A. Holm, W. S. Foster, G. R. Loefer
Engineering Experiment Station
Georgia Institute of Technology
Atlanta, Georgia 30332

ABSTRACT

A combined electro-optical/millimeter wave radar sensor system is described and the results of preliminary field tests with this system are presented. The electro-optical sensor is a conventional television camera. Future modifications of this system, which includes installing a pulsed laser radar as the electro-optical sensor and future plans for this program are discussed.

I. INTRODUCTION

Tactical surveillance and weapon guidance systems depend critically on the Army's ability to not only acquire, but also to identify and to precisely locate targets of military significance. Conventional microwave radars have traditionally fulfilled the target acquisition role for the Army. However, due to resolution limitations inherent in the microwave frequency domain, these radars have met with limited success in target identification and precise target location required for accurate weapons delivery. To overcome these inherent inadequacies in radar systems, there has recently been a rapid emergence of electro-optical (EO) sensors, such as low-light-level television, forward looking and other infrared sensors and laser radar. Since these devices operate at, or are sensitive to, frequencies in the infrared to visible region of the electromagnetic spectrum, they have a much greater resolution than that of microwave radars and thus are able to more adequately fulfill the target identification and precise target location roles.

Two basic limitations of EO sensors prevent these sensors from completely replacing the radar sensor in tactical operations. First of all, EO sensors are inadequate in a search and target acquisition role due to the length of time needed for these extremely high resolution sensors to scan a given spatial volume. Secondly, EO sensors suffer much higher atmospheric

attenuation losses than microwave sensors, especially in degraded weather conditions or in a smoke, fog or aerosol environment. Under these atmospheric conditions and without a microwave radar aboard, an Army vehicle, e.g., tank, would literally be "blind" to its surroundings.

To overcome the individual inadequacies of the two sensor systems and at the same time take advantage of their respective capabilities and strengths, both sensors can be utilized together in an augmenting fashion to form a combined electro-optical/radar sensor system. With this in mind, the Engineering Experiment Station (EES) at the Georgia Institute of Technology recently began a multi-phase program under contract with the U. S. Army ERADCOM to demonstrate the feasibility of such a combined EO/millimeter wave radar sensor system. In this dual sensor system, the millimeter wave radar system performs its conventional role of searching large spatial volumes in order to acquire and crudely locate a target. Once the target is acquired, the higher resolution EO sensor is directed toward the target for identification, accurate and precise target location and weapons delivery.

The ultimate goal of the program is to have for the EO sensor a pulsed, heterodyned CO_2 laser radar suitable for weapon guidance. In Phase I of the program, which is nearing completion, basic interfacing problems between the two sensors are being investigated. A conventional television camera (vidicon) and monitor are being used to simulate the laser radar. In this paper, the preliminary results of this initial phase of the program are discussed and the plans for future phases are reviewed. In Section II, the combined EO/millimeter wave sensor system itself is discussed. In Section III, Phase I of the program is discussed, the results of the preliminary field tests with the combined sensor system are presented and some of the EO/Radar interfacing problems discussed. Finally, in Section IV, future plans for the program, including those involving the laser radar sensor, are reviewed.

II. EO/MILLIMETER WAVE RADAR SENSOR SYSTEM

The radar system used in the combined dual sensor system is Georgia Tech's 70 Ghz (4.3 mm), high-resolution, rapid scan radar originally built by EES for Harry Diamond Laboratories. This radar was made mobile by installing it in a M-109 shop van. The radar console and antenna are linked together and revolve about a common axis. The operator faces the direction illuminated by the radar and a periscope, whose optical axis is aligned with the antenna electromagnetic axis, provides him with an optical view of the illuminated area. The basic system parameters of this radar are given in Table I.

The radar antenna assembly was recently modified by the addition of two microwave reflectors (see Figure 1). When in use, these reflectors essentially rotate the microwave beam through 90° upon leaving the antenna, thus enabling the radar to operate in a vertical scan mode. To activate the vertical scan mode, the tiltable plane reflector-mirror assembly (see Figure 2) must be folded back toward the antenna so that the microwaves can reach

the vertical scan reflectors. While in the vertical scan mode, the EO sensor is inoperative.

The EO sensor is a conventional television (TV) camera (vidicon) which is mounted in the van and aligned with the periscope so that the EO optical axis and radar microwave axis are mechanically co-boresighted in azimuth (see Figures 2 and 3). Attached to the camera is a lens with variable magnification from x15 to x60 corresponding to a field-of-view from approximately 14.2 mrad to 3.5 mrad. Another TV camera is focused on the radar display and the outputs from the two cameras are fed into a special effects generator which in turn is connected to a video tape recorder and monitor (see Figure 4). Thus, the radar display and optical imaging can be displayed together in a "split-screen" effect.

III. PHASE I OF THE PROGRAM AND RESULTS OF THE PRELIMINARY FIELD TESTS

A. Phase I of the Program

In Phase I of the program, basic interfacing problems between the two sensors are being investigated. These problems include:

1. Determination of the minimum angular uncertainty in target location achievable with the radar sensor alone, and
2. Determination of the best method of coupling the two sensors together.

The basic target locating accuracy of the radar in a clutter and multipath environment is of critical importance in determining the field-of-view (FOV) to be scanned by the laser radar. Because of the large amount of time required by the laser to scan large spatial volumes, the FOV must be kept to a minimum. Therefore, a determination must be made of the minimum angular uncertainty in target location achievable with the radar.

There are several ways to "handoff" from the radar to the EO sensor, i.e., several methods of coupling the two sensors together. These methods vary from a system where the laser sensor is on a set of gimbals and is electronically coupled to the radar, to a system where the coupling is done both electronically and mechanically, to a totally mechanically coupled system. As was mentioned in Section II, for feasibility demonstration purposes the EO sensor is currently mechanically coupled to the radar in azimuth with no coupling in elevation.

B. Results of the Preliminary Field Test

Preliminary calibration/shake-down field tests of the combined EO/Radar sensor were conducted at Ft. Gillem, Georgia on 20-30 Sept., 1977. The tests were conducted in a field with relatively flat terrain bounded with trees on either side and with a range of over 1200 meters.

The beamsplitting experiments consisted of simply having the radar ope-

rator center the azimuth or elevation cursor on the target return as displayed on a B-scope. The angular placement of the cursor was then compared to the true angular position of the target as measured with a theodolite located in the antenna assembly. No attempt was made on these initial series of field tests to eliminate the human factor and its affect on the test results. Targets included both corner reflectors and a small pick-up truck. Results of these tests are summarized in Table II. Within one standard deviation, a target could be located in both azimuth and elevation to an accuracy of approximately 1 mrad. Given the radar's 9.6 mrad beamwidth, this represents roughly a 9:1 beamsplit.

Finally, to demonstrate the overall feasibility of combining an EO sensor with a radar sensor, several "handoff" experiments were performed. The EO and radar boresights were aligned and then several targets were acquired by the radar. Once a target had been acquired and aligned on the radar's boresight, the EO sensor was activated to determine whether or not the target was in the EO sensor's FOV, and if so, to identify the target. During these tests, the EO sensor was kept at its maximum FOV. The combined sensor system performed very well during these tests with the target being well centered on the monitor. Several video tape recordings were taken from which two still frames are shown in Figures 5 and 6.

IV. FUTURE PLANS FOR THE PROGRAM

In the remainder of Phase I of the program, which will terminate on 31 Jan. 1978, extensive field tests will be conducted in which the minimum angular uncertainty in target location achievable with the radar will be precisely determined. This data will be operationally checked by actually conducting various "handoff" experiments in which the FOV of the TV camera will be varied in order to simulate different possible FOV's being scanned by the laser sensor. In this way, the actual FOV to be scanned by the laser sensor can be determined. Based on preliminary results, a 3 mrad FOV is currently being planned. In addition, a determination will be made in this phase of the program as to the best method of coupling the two sensors together.

In Phase II of the program, which is already underway, a CW CO_2 laser sensor system will be constructed and integrated with the radar. Within the next three months this integration will be completed, with a He-Ne laser simulating the CO_2 laser. In four to six months, a CW direct detection system will be operative with:

1. a 5 watt CW CO_2 laser,
2. a resolution cell of 0.1 mrad, total FOV 1 mrad
3. a frame rate of 20 hz

In 10 to 18 months, a CW heterodyned receiver will be operative with a second laser as L.O.

In Phase III of the program, a pulsed, heterodyned CO_2 laser radar will be developed as the EO sensor. This sensor will have a 5 KW or greater peak power, 18 Khz PRF and a CW laser as L.O.

ACKNOWLEDGMENTS

The authors wish to acknowledge the following people for their contributions to this program: N. T. Alexander, J. E. Davidson, J. A. McKenzie and S. Y. Willis.

TABLE I. BASIC RADAR SYSTEM PARAMETERS

1. ANTENNA: FOLDED, GEODESIC LENS FEEDING A PARABOLIC CYLINDER REFLECTOR. THE ANTENNA IS 25 INCH DIAMETER BY 3.5 INCH HEIGHT. GAIN: 43.2 dB (CORRECTED FOR LOSS)

2. SCANNING MODES: SCANNING BY A SEVEN RING SWITCH WHICH ALLOWS A SCAN RATE OF APPROXIMATELY 1 RPM TO 50 RPS

   AZIMUTH SCAN MODE:

   SCAN ANGLE: 45° (±22.5° ABOUT BORESIGHT)
   AZIMUTH BEAMWIDTH: 0.55° (POSITIONABLE THROUGH 360°)
   VERTICAL BEAMWIDTH: 3.5° (POSITIONABLE FROM -10° TO 20°)

   VERTICAL SCAN MODE

   SCAN ANGLE: -5° TO 10° (APPROXIMATELY)
   AZIMUTH BEAMWIDTH: 3.5° (POSITIONABLE THROUGH 360°)
   VERTICAL BEAMWIDTH: 0.55° (POSITIONABLE THROUGH ±5°)

3. TRANSMITTER:

   MAGNETRON: BOMAC BL 234C
   PEAK POWER: 500 WATTS
   FREQUENCY: 69 TO 71 GHz
   RF PULSE WIDTH: 20 AND 45 NANOSECONDS (ADJUSTABLE)
   PULSE REPETITION FREQUENCY: 5 KHz TO 25 KHz (VARIABLE)
   MODULATOR: TRIGGERED BLOCKING OSCILLATOR
   DUPLEXER: BOMAC BL-P-017D

4. RF COMPONENT LOSS: 6 dB (TOTAL)

5. LOCAL OSCILLATOR: VARIAN VA 250 KLYSTRON

6. MIXER: PHILCO IN2792 MIXER CRYSTAL; CONVERSION LOSS 15 dB
   EQUIVALENT NOISE FIGURE 18 dB MINIMUM
   EQUIVALENT NOISE FIGURE WITH IF 25 dB MAXIMUM

7. IF: GAIN: 70 dB
   CENTER FREQUENCY: 400 MHz
   BANDWIDTH: 60 MHz
   NOISE FIGURE: 5 dB

8. VIDEO AMP:

   BANDWIDTH: 50 MHz
   GAIN: 150 (VOLTAGE)

9. DISPLAYS-INDICATOR UNITS:

   SECTOR SCAN
   B-SCAN MODE
   NON-COHERENT DOPPLER AURAL DISPLAY

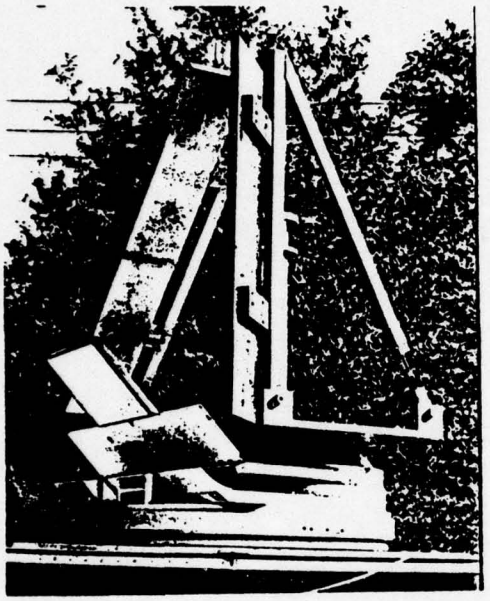

Figure 1. 70-Ghz Antenna Assembly With Vertical Scan Reflectors Mounted On Top Of Geodesic Lens Antenna

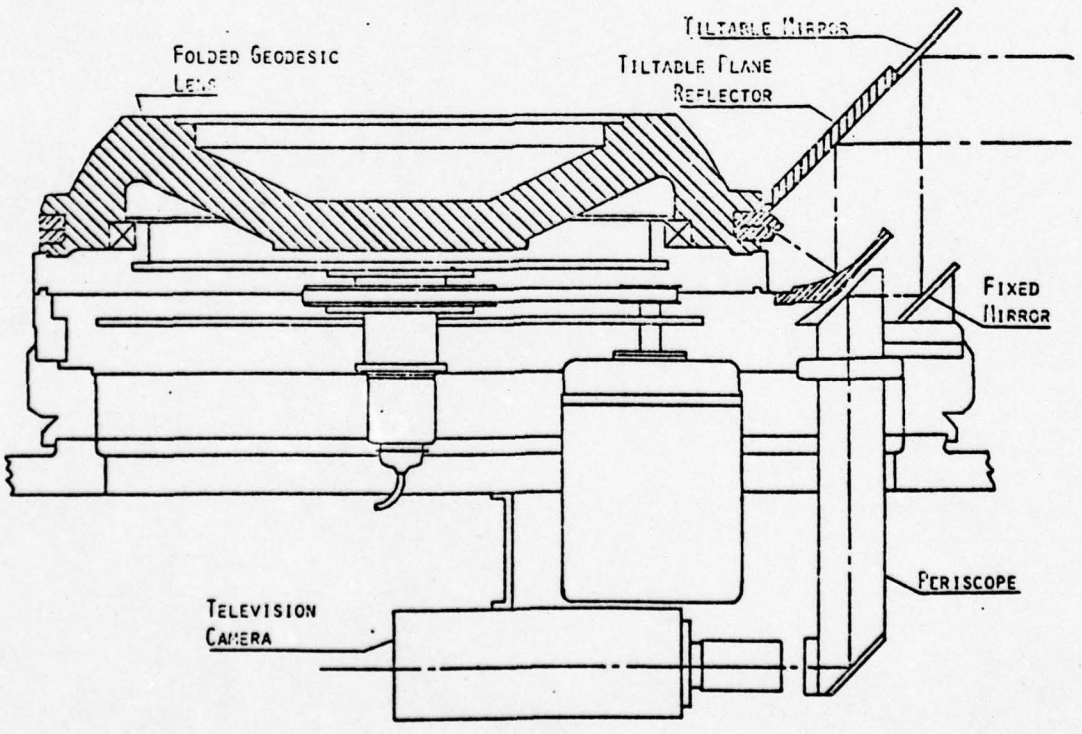

Figure 2. 70-Ghz Folded Geodesic Lens Antenna With TV Camera Mounted For Viewing Through Periscope

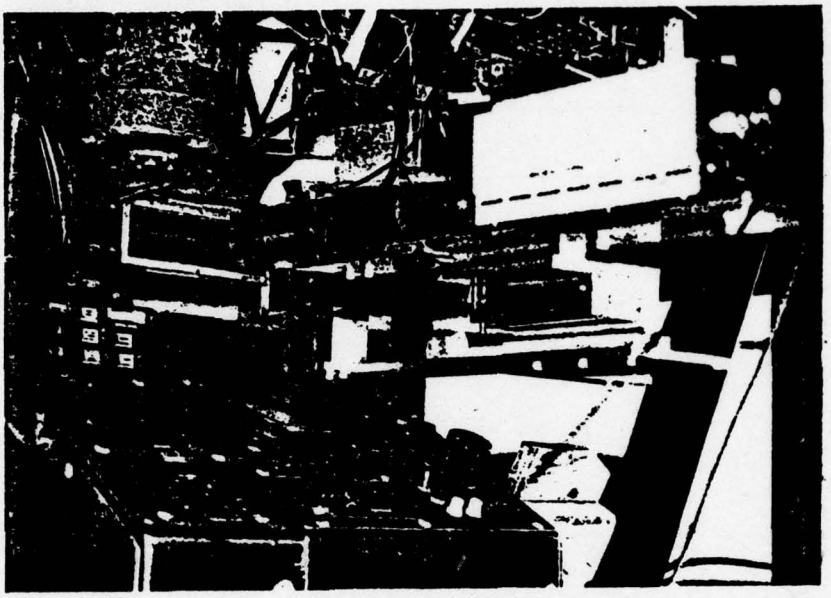

Figure 3. TV Camera Aligned With Periscope And Radar Display And Controls (2nd TV Camera Not Shown)

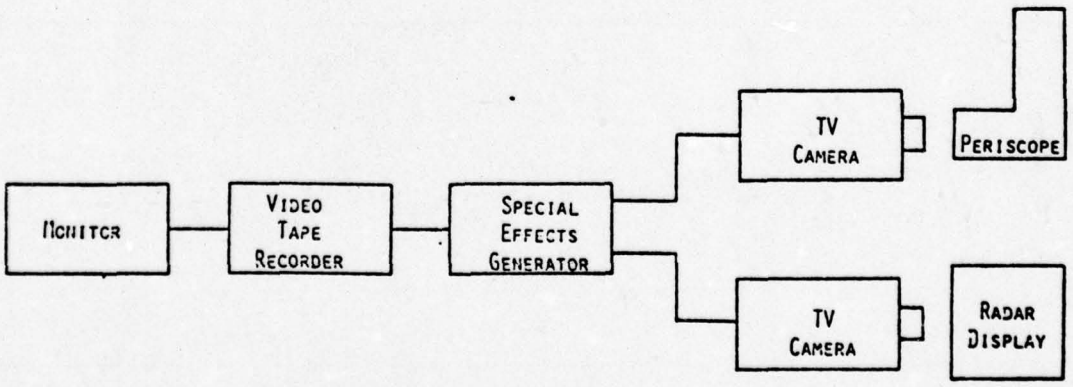

FIGURE 4. SCHEMATIC DRAWING OF EO/RADAR MONITORING AND RECORDING SYSTEM

TABLE II. BEAMSPLITTING RESULTS FROM PRELIMINARY FIELD TESTS

ELEVATION BEAMSPLITTING

TARGET	NO. OF TRIALS	RANGE (M)	RESOLUTION (ONE STANDARD DEVIATION)
CORNER REFLECTOR	30	168	1.047 MRAD
CORNER REFLECTOR	30	168	1.066 MRAD
TRUCK	6	112-408	0.544 MRAD
TRUCK	8	455-1026	1.009 MRAD

AZIMUTH BEAMSPLITTING

TARGET	NO. OF TRIALS	RANGE (M)	RESOLUTION (ONE STANDARD DEVIATION)
CORNER REFLECTOR	30	356	1.117 MRAD

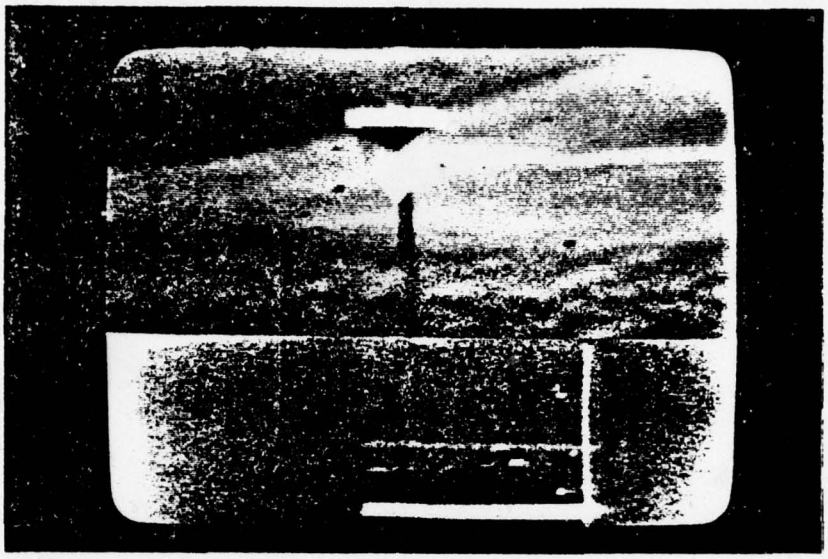

Figure 5. Still Frame Photo Of Video Tape Recording Showing Split Screen Of Corner Reflector As Simultaneously Imaged By EO Sensor (Top) And Displayed By Radar On B-Scope

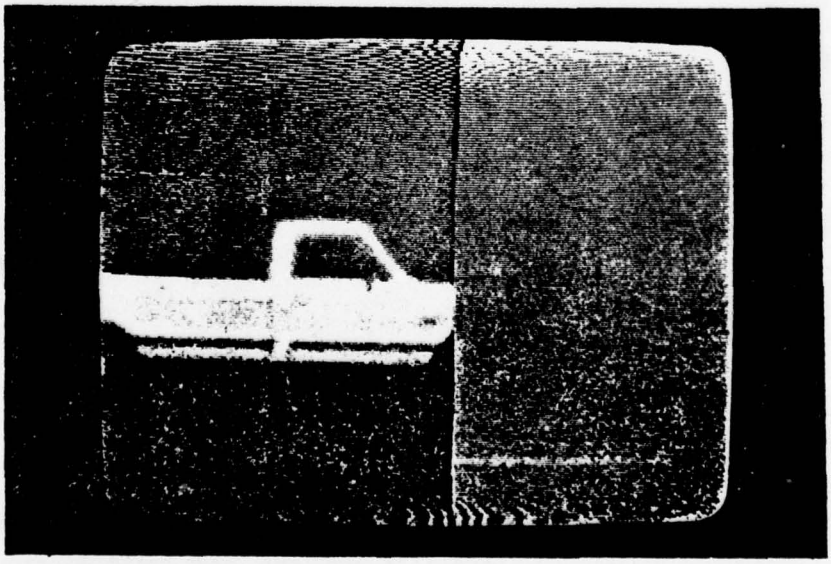

Figure 6. Still Frame Photo Of Video Tape Recording Showing Split Screen Of Truck As Simultaneously Imaged By EO Sensor (Left) And Displayed By Radar On B-Scope

APPENDIX II

Paper Presented To:

Workshop on Millimeter and Submillimeter
Atmospheric Propagation Applicable to Radar
and Missile Systems

"Measurements of Attenuation Due
to Simulated Battlefield Dust
at 94 and 140 GHz"

Presented To
Workshop on Millimeter and Submillimeter Atmospheric
Propagation Applicable to Radar and Missile Systems

MEASUREMENTS OF ATTENUATION DUE TO SIMULATED BATTLEFIELD DUST AT 94 AND 140 GHz*

J. J. Gallagher, R. W. McMillan, and R. C. Rogers

Georgia Institute of Technology
Engineering Experiment Station
Atlanta, Georgia 30332

Donald E. Snider

U. S. Army Atmospheric Sciences Laboratory
White Sands Missile Range, New Mexico

ABSTRACT

During the fall of 1978, a series of measurements, called DIRT I, of electromagnetic wave propagation through simulated battlefield dust were conducted at White Sands Missile Range. This paper gives an overview of the entire DIRT I tests as well as detailed results of those tests for millimeter wave (94 and 140 GHz) frequencies.

Attenuation measurements were made over an instrumented 2 km range. In the center of the range, explosive charges of different sizes were detonated, and the resulting signal level was compared to that existing before the explosive event. Measurements were also made of attenuation caused by artillery shells fired into the center of the range, and of that caused by burning diesel oil and rubber.

Both magnitude and duration of attenuation were found to vary with the amount of the explosive, sometimes reaching 30 dB and 20 seconds respectively. Copies of chart recorder tracings showing attenuation of both explosion products and oil smoke are presented. Oil smoke propagation measurements show scintillations of 3 to 5 dB.

1. INTRODUCTION

Battlefield obscurants such as dust and smoke from vehicle activity, burning wreckage, or explosion debris from artillery impacts can cause serious degradation in the performance of electro-optical (EO) weapon and surveillance systems. Individuals actively involved in the development of EO sensor systems realize that evaluating the performance of these systems under degraded atmospheric propagation conditions expected on the battlefield requires solutions to scientific and engineering problems of staggering difficulty. The extreme complexities of the natural atmosphere, the differing soil properties throughout the world, seasonal and meteorological variations, different types and different applications of military munitions, and the engineering details of EO systems themselves all combine to produce an endless list of problems to be solved. Some combination of empirical and theoretical investigations must be made to sort out these problems and to find solutions to the extent needed to permit an operationally adequate estimate of weapon system performance under realistic battlefield optical conditions. With this in mind the Dusty Infrared Test - 1 (DIRT I) was conceived as the beginning of a direct contribution toward the solution. The primary objectives of DIRT I were to provide a developmental test of some of the technology which must be brought to bear on the problems, such as lidars, soil analyses, FLIR images, aerosol samplers, transmissometers, and others together in a coordinated program to produce information of direct use to the EO sensor and obscuration modeling communities; to characterize the dust cloud produced by various amounts of high energy explosives; and to obtain data for the development of scaling laws. A detailed report on DIRT I has been prepared by the Atmospheric Sciences Laboratory [Lindberg, 1979].

In order to perform this first set of experiments, ASL assembled investigators from several organizations at the White Sands Missile Range to participate in the observations. Thus, for measuring aerosol particulate sizes, a large instrumented payload was suspended from a CH54 "Skycrane" helicopter and flown through the explosion cloud for direct sensing of the dust properties. Several measurements of the effects of the explosion dust on electro-magnetic transmissions were made. The Naval Research Laboratory performed bandpass filter and Fourier Transform Spectrometer transmission measurements; Stanford Research Institute provided lidar measurement support; and Georgia Tech performed millimeter wave transmission measurements. Excellent support was also provided by the U. S. Army Waterways Experiment Station (soil characterization and explosion crater data), the U. S. Army 3rd Armored Cavalry Regiment (155 - mm howitzer firings), the 14th Aviation Batallion, 273rd Transportation Company (CH54 helicopter support), the White Sands Missile Range Explosive Ordinance Demolition team (planning, installing and detonating the explosive arrays), and the U. S. Army Text and Evaluation Command elements at WSMR (gas sampling data, photography and general range support). The propagation measurements were performed by transmitting

*Lindberg, 1979

through TNT explosions, explosions from static 155 - mm rounds and live artillery firings. This presentation discusses the millimeter wave propagation tests.

2. Description of Test Site

The DIRT I tests were conducted by ASL between 2 and 14 October 1978 in the southeast corner of White Sands Missile Range (WSMR), New Mexico. Figure 1 shows the orientation of the DIRT I test area and the locations of the test area and the major instrumentation and support sites. Figure 2 illustrates the detailed layout of the DIRT I site and location of experiments and equipment. The distance between the south site and north site was 2 kilometers. The test area, 100 by 300 meters was situated midway along the path and was the location of all detonations and artillery impacts. The path was cleared of vegetation to a width of approximately 20 meters.

3. DIRT I Events

The simulated battlefield dust was generated by detonating TNT charges, static detonation of 155 mm projectiles and live firings of 155 mm howitzers. The detonation events were performed as indicated in Figures 3 through 8. Each event was designated as A - 1, A - 2, etc. through E - 10. Events A - 1 through D - 4 were detonations of charges of TNT laid as shown in Figures 3 through 6. The E - events (Figures 7 and 8) were static detonations of 155 - mm howitzer projectiles. The positions of the projectiles for the E - events are illustrated in Figure 9.

The F - events were live howitzer firing events with four 155 - millimeter howitzers firing at one point in the impact area. Event F - 1 consisted of firing one round from each of the four 155 - mm tubes simultaneously into the impact area. Events F - 2 and F - 3 were similar, except each tube delivered 3 rounds in a time interval of about 45 seconds for a total of 12 rounds. Events F - 4 through F - 7 were similar except that 8 rounds were fired. Three projectiles were fired for F - 8.

The last event in DIRT I was a fuel fire. For this test, four 55 - gallon steel drums were cut in half and laid in a trench perpendicular to the optical axis in the center of the test area. Thirty-eight liters of diesel fuel, two liters of motor oil, and one rubber tire were placed into each container. The mixture was ignited and produced great volumes of black smoke for the duration of the test, approximately 37 minutes. The payload was flown through the cloud 11 times at various heights above the ground while simultaneous transmission measurements were being made by ground-based sensors.

4. Millimeter Wavelength Transmission Measurements

A potentially severe problem in the use of millimeter waves in battlefield situations is the possible degradation of these systems caused by atmospheric propagation effects. Some fairly extensive studies and measurement programs have led to some understanding of the performance of millimeter systems in rain and fog, although much work remains to be done in this area, but little work has been done to characterize millimeter propagation through battlefield dust. This discussion gives the results of a series of experiments conducted during DIRT I by personnel of the Georgia Tech Engineering Experiment Station in October 1978 which attempt to fill this gap in knowledge about millimeter wave propagation.

During most of the experiments, simultaneous measurements were made at 94 - and 140 - gigahertz; however, a power supply failure caused the 140 - gigahertz receiver to become inoperative. Therefore, only 94 - gigahertz measurements were obtained during some of the events.

The simulated battlefield dust was generated by detonating TNT charges, static detonation of 155 - millimeter howitzer projectiles, and live firings of 155 - millimeter howitzers. In addition, an event was conducted on the final day which measured signal degradation caused by simulated burning vehicles. The aerosols generated during most of the above events were characterized by a helicopter - borne sensor package.

Block diagrams of the 94 - and 140 - gigahertz transmitter/receiver systems are shown in Figures 10 and 11 respectively. Both of these systems use CW klystrons that are chopped at a 1 - kilohertz rate for phase sensitive detection. Both also use superheterodyne receivers for good sensitivity.

The 94 - gigahertz transmitter uses an OKI 90V11 klystron which has a power output of about 80 milliwatts. The antenna is a horn/lens combination which has a beam width of 2 degrees. Part of the power is picked off with a directional coupler to monitor transmitter power and frequency through a wavemeter, detector, and oscilloscope. The klystron is 100 percent modulated with a 1 - kilohertz square wave applied to its reflector from the internal power supply modulator, whose output is also used to modulate the 140 - gigahertz tube, so that only one reference signal for phase sensitive detection need be transmitted. This signal is transmitted to the receiver over twisted pair lines by means of line drivers and receivers.

The 94 - gigahertz receiver uses a gallium arsenide Schottky barrier diode mixer pumped by a Varian VRB - 2113AB klystron local oscillator (LO). Signal and LO power are coupled into the mixer by a cylindrical coupling cavity. For most of the events, two Avantek 1 to 2 megahertz IF amplifiers were used, but for the first few events one Avantek 1 to 2 megahertz amplifier and one Watkins - Johnson 5 to 1000 - megahertz amplifier were used. Each of these amplifiers has a gain of 30 decibels, so that the IF gain was 60 decibels total. An identical amplifier arrangement was used on the 140 - gigahertz system; but after a power supply failure caused this system to be inoperative, both Avantek amplifiers were used with the 94 gigahertz receiver.

The output of the IF amplifier is fed into a zero-bias tunnel diode detector, which is the signal input for a lock-in amplifier. The output of this amplifier drives a strip chart recorder which shows the variations in signal as

a result of the explosions.

The 140 - gigahertz transmitter tube is an OKI KA1390 klystron with an out-put of about 40 milliwatts. A tunable Fabry - Perot interferometer was used to measure the frequency of this tube and a Sharpless wafer mixer-detector with a corrugated horn was used to monitor its power. This tube was modulated with the same signal used to modulate the 94 - gigahertz tube.

The 140 - gigahertz receiver consists of a gallium arsenide Schottky barrier diode harmonic mixer in a crossed waveguide mount. This mixer is pumped by an OKI 70V11A klystron which oscillates at 70 gigahertz. The IF amplifier arrangement is that discussed in the paragraph which treats the 94 - gigahertz receiver. The second detector, lock-in amplifier, and chart recorder are also used in the same way as discussed earlier for that receiver.

The measurements were calibrated both before and after the events. For the 94 - gigahertz system, a precision attenuator between the transmitter tube and the antenna was used. Generally, measurements were calibrated at 0 -, 3 -, 6 -, 9 -, and 12 - decibel levels. In comparing the results of event measurements to these calibrations, a curve was plotted which showed attenuation as a function of chart recorder displacement. The true attenuations due to the event could then be scaled from the curve. This method corrects for any nonlinearities or departures from square law in the superheterodyne receiver. A precision attenuator was not available for the 140 - gigahertz system, so it was calibrated by obtaining output readings for zero and infinite attenuation and scaling measured results linearly. This method assumes, of course, that the receiver is a true square law detector.

5. Discussion of Events

The results of only a few events will be discussed here. The C - events were the large simulated barrages of 140 charges of 15 pounds each. Figure 12 shows the results obtained during event C - 1. Both 94 - and 140 - gigahertz channels exhibit attenuations of greater than 28 decibels. Recovery time of both systems was determined to be greater than 20 seconds. Note however that the 94 - gigahertz channel recovers to within 3 decibels of its original level in about 8 seconds, while the 140 - gigahertz channel requires about twice as long due to a large secondary minimum at about 12 seconds. Note also that the scintillation amplitude for both channels is smaller for this event. For this event, the system was operated with zero time constant. The dynamic range of the system amplifiers did not allow an exact determination of attenuation other than that it was greater than 28 decibels. The large minimum for 140 gigahertz in the region of 7 to 11 seconds was apparently a zero shift as the signal did not return to the original zero and no corresponding effects are observed on the 94 - gigahertz trace. Equipment problems prevented accurate measurements for the similar event, C - 2. It was estimated that, by changing scales on the lock - in and recorder, the attenuation at 94 gigahertz exceeded 35 decibels. No accurate rate time estimates could be made because of the equipment difficulties.

All events showed attenuation characteristic of the size of the explosion ranging from approximately 6dB maximum attenuation to 35 dB maximum attenuation. In all observations, recovery time for events B through E did not exceed 25 seconds.

The F - events are the remote howitzer firings and attenuation is strongly dependent on whether or not the rounds land on the road which is the millimeter wave transmission path. For example, the events corresponding to events F - 1 and F - 4 show no attenuation. However, the howitzer round did not land in the center of the test area. Figure 13 shows measurements made during event F - 2 of 12 October 1978. This firing consisted of three groups of four 155 - millimeter howitzer rounds. These three groups occur in the time range of 12 to 45 seconds. The peak at approximately 51 seconds is a single round that should have been included in the group at 43 seconds.

The measurements on 12 October through 14 October 1978 were overdriven and as a result gave nonlinear calibration. This can be seen from Figure 14 where it is evident that the greater power employed also resulted in a reduction of scintillation when explosions were not occurring. From Figure 14, the 0 - decibel level is the original level; but drift occured during the firing, resulting in a different baseline. This incident occured in several events during the last 3 days.

Note that on some rounds positive peaks were obtained which possibly corresponded to reflection of transmitter signal into the receiver antenna. Some of the attenuation peaks were on the order of 20 decibels. The recovery time cannot be ascertained accurately because of the spread of impact times, but recovery appears to be complete within 10 to 12 seconds after the last impact. Figure 15 shows the measurements of event F - 3 of 12 October 1978. The event was again three firings of four howitzer rounds. The first group which should have produced attenuation at 15 to 20 seconds did not record an effect, possibly as a result of the firing missing the test area. Figure 16 shows two groups at 35 to 40 seconds and 48 to 57 seconds; the amplitude of these groups is significantly reduced (3 to 4 decibels) relative to F - 2.

A second series of F events was run on 13 October 1978. Again during event F - 8 no attenuation was measured, probably as a result of the rounds missing the test area. Results obtained during event F - 5 are given in Figure 16. This recorder trace corresponds to two firings of four rounds each with peak attenuations of 10 decibels and approximately 6 decibels. For Figure 16, the chart recorder speed was set at 15 centimeters per minute, too slow to show very much detail. Recovery is within about 4 seconds for the first maximum. The second salvo of this event apparently did not land precisely in the line of sight because the maximum attenuation is 6 decibels and the recovery time is less than 1 second.

Event F - 6 of 13 October is shown in Figure 17. The maximum attenuation observed for this

event was approximately 6 decibels with recovery in 3 to 4 seconds. The chart recorder speed was increased to 1.25 centimeters per second to show more detail for this test. An interesting phenomenon occurs in both salvos of this event in which the attenuation actually goes negative. This may possibly be caused by multipath scattering from shell fragments.

The results obtained for event F - 7 are given in Figure 18. Maximum attenuation for both salvos was determined to be 9 and 8 decibels with recovery times of about 4 to 5 seconds. For this event, the absorption did not invert and was stronger than in event F - 6. The stronger absorptions of F - 7 are consistent with the impacts being more directly in the optical path than F - 6 with a corresponding reduction of scattering into the receiver.

On Saturday, 14 October 1978, a test was conducted in which diesel fuel, motor oil, and rubber, in the approximate ratios expected in a burning tank, were utilized to simulate a "burning hulk." The paper chart depicting 94 gigahertz transmission as a function of time (about 45 minutes) is published in reference 1.

As might have been expected, the bulk average attenuation during this test was relatively small--on the order of 1 or 2 decibels. However, scintillations of up to 5 decibels peak were observed. The frequency spectrum of these scintillations appears higher than that observed for purely atmospheric scintillations, and the amplitude is also greater.

Unfortunately, the signal was not recorded on magnetic tape. Thus a power spectrum analysis cannot be readily performed. Such an analysis would be important in quantitatively determining the effects of these scintillations on millimeter wave systems.

6. Conclusions and Recommendations

DIRT I has provided an opportunity for observing the effects of tactical size explosions on millimeter wave and electro-optical propagation. In many events, attenuations of 10 to 30 decibels were observed. Although damage suffered by equipment in transit caused some limitations and eventual failure of the 140 - gigahertz apparatus, generally significant data were obtained.

Several conclusions can be drawn from the measurements. As indicated, attenuation in most cases was large. The relatively short recovery time of the attenuated signal indicates that the attenuation was caused by the large pieces of soil blown in the air in the early stage of each event. The residual dust remaining in the air after the initial large particles have settled makes no significant contribution to the attenuation. This result is similar to the results obtained at millimeter wavelengths when propagating through dust raised by vehicles. The signal fluctuations in the majority of the events were large, and their origin has not been fully established. As indicated by the monitoring of the source amplitude stability and the receiver noise level when signal is blocked, the fluctuations probably do not receive a major contribution from the instrumentation. Some contribution could originate from atmospheric fluctuations. Quite probably, the majority of these fluctuations result from multipath effects.

The large beam widths (2 degrees) resulted in effects from vehicles, personnel, moving bushes, etc., being observable in the receiver system. A more narrow beam antenna system would minimize these effects. The fluctuations which were observed were of sufficient magnitude to obscure small attenuation effects. Frequency stability of the transmitter and local oscillator was sufficient to keep the signal within the amplifier bandwidth and thereby cause no fluctuations.

The scintillation during the burning of the diesel oil, motor oil, and rubber was large and exceeded the expected effect.

The signals obtained during the howitzer firings varied significantly for each event. The strength of the absorption depended on the position of the impact relative to the optical path of the system. The spread in absorption for each salvo resulted from the difference in time for the impact of each round. The positive signal response which was observed for some firings appeared to result when attenuation was not the greatest and probably when the impact area was not directly in the optical path. As a result, scattering of signal into the receiver by the fragments blown in the air may possibly have been the cause of signal increase.

DIRT I has provided a great deal of tranmission data that were collected along nearly identical propagation paths. Detailed data reduction from all systems and careful consideration of possible extenuating circumstances, e. g., detector linearity, are not yet complete. However, quick-look data are sufficient to draw some tentative conclusions. An example is shown in Figure 18. In this figure the results from the 0.55- and the 10.35 - micrometer Naval Research Laboratory filter transmissometers, measurements of transmission obtained from the Atmospheric Sciences and Stanford Research Laboratories' lidars, and the Georgia Institute of Technology 94 - gigahertz transmissometer are intercompared for event F - 2. It is clear that for the visible and infrared wavelengths an artillery barrage can produce attenuation of 15 or 20 decibels for periods of several minutes and that, at least for a desert soil in New Mexico, the signal recovery is not significantly better for any particular visible or infrared wavelength. The attenuation at 94 - gigahertz was larger than anticipated but existed for a shorter period. Nevertheless even at this early stage in data examination, it is possible to conclude two things from data such as those in Figure 18. One is that a 155 - millimeter barrage can seriously obscure infrared propagation for periods of several minutes, and the second is that even a 94 - gigahertz signal can suffer attenuation greater than 10 decibels for periods of a few seconds.

7. Acknowledgement

The authors wish to acknowledge the support of J. D. Lindberg, Test Director, R. Loveland, Deputy Test Director and B. W. Kennedy, Test Conductor and the assistance of R. Platt and D. Guillory, Georgia Tech students who helped in the measurement programs. This work was supported by the U. S. Army Atmospheric Science Laboratory through Army Research Office Contract

No. DAAG 29 - 77 - C - 0026.

1. J. D. Lindberg, "Measured Effects of Battlefield Dust and Smoke on Visible, Infrared, and Millimeter Wavelength Propagation; A Preliminary Report on Dusty Infrared Tests - I (DIRT I)," ASL - TR - 0021 (Atmospheric Sciences Laboratory, White Sands Missile Range, NM 88002), January, 1979.

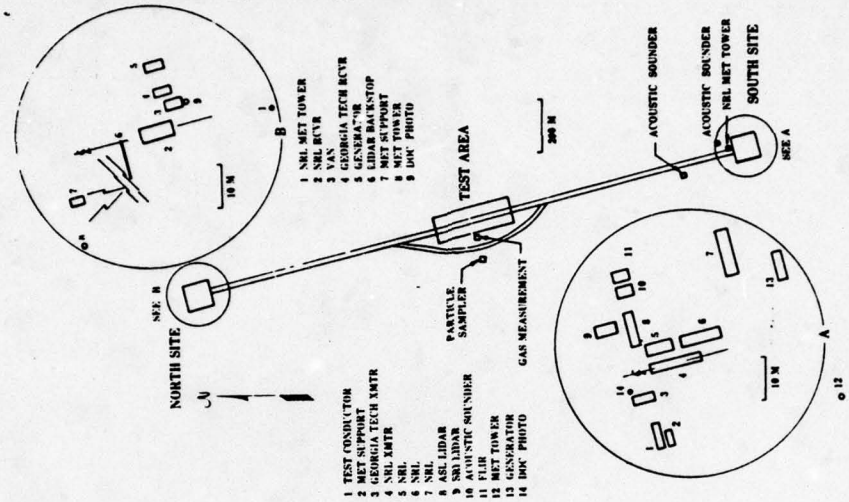

Figure 2. Detailed layout of DIRT I site showing locations of vans and experiments at each end. Path length from north to south is 2 km. Test area, where explosives were detonated and artillery shells impacted, is 100 by 300 m.

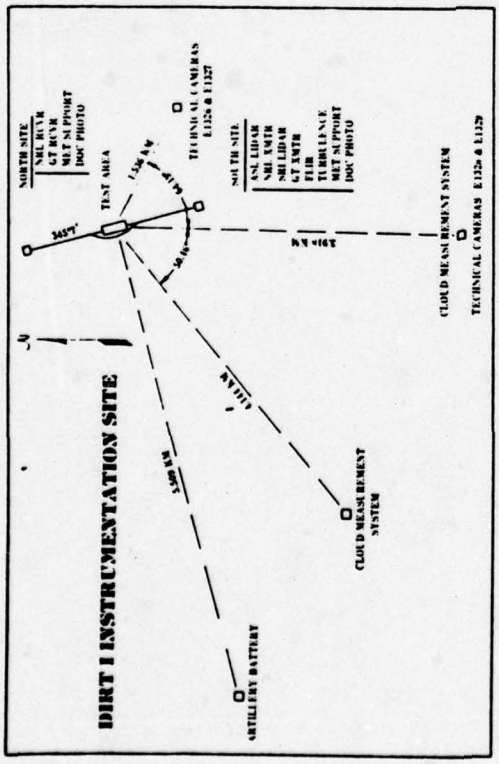

Figure 1. Plane view of DIRT I site showing remotely located instrumentation and support elements. General location is in extreme southeast corner of White Sands Missile Range, New Mexico.

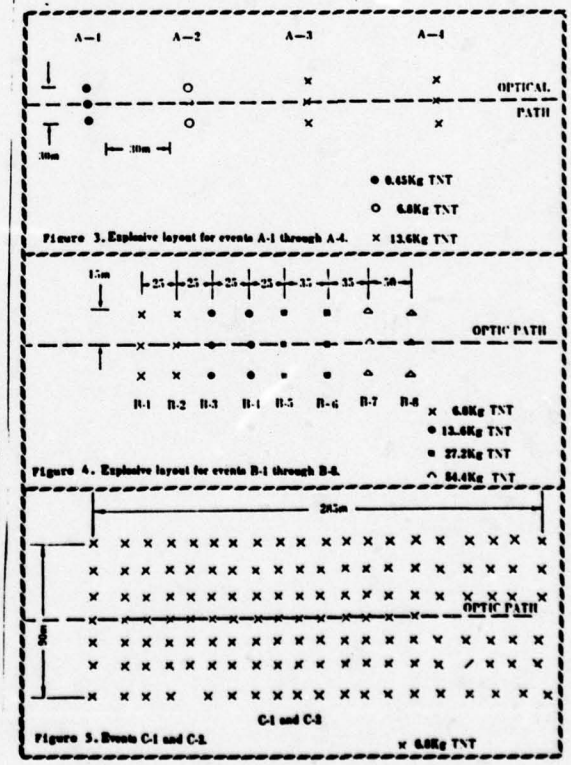

Figure 3. Explosive layout for events A-1 through A-4.

Figure 4. Explosive layout for events B-1 through B-8.

Figure 5. Events C-1 and C-2.

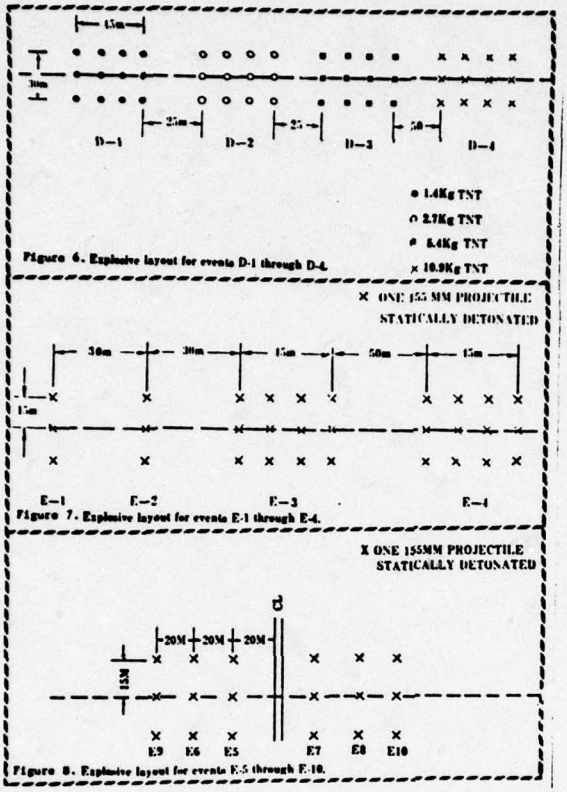

Figure 6. Explosive layout for events D-1 through D-4.

Figure 7. Explosive layout for events E-1 through E-4.

Figure 8. Explosive layout for events E-5 through E-10.

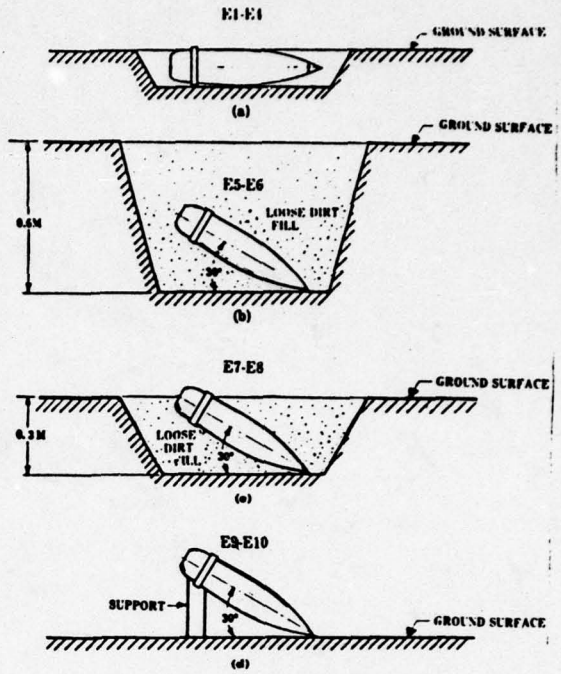

Figure 9. Altitude of 155 - mm projectiles in ground for events E - 1 through E - 10: (a) events E - 1 through E - 4, (b) E - 5 and E - 6, (c) E - 7 and E - 8, (d) E - 9 and E - 10.

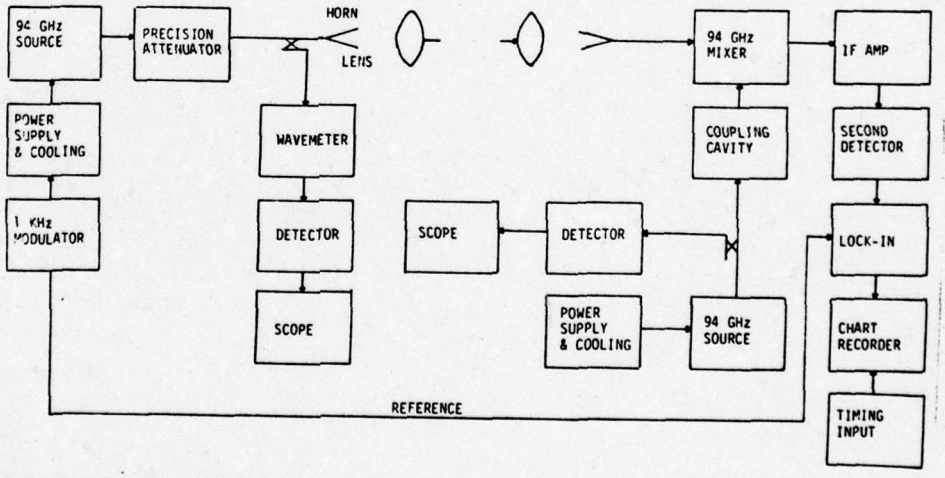

Figure 10. 94 gigahertz system block diagram.

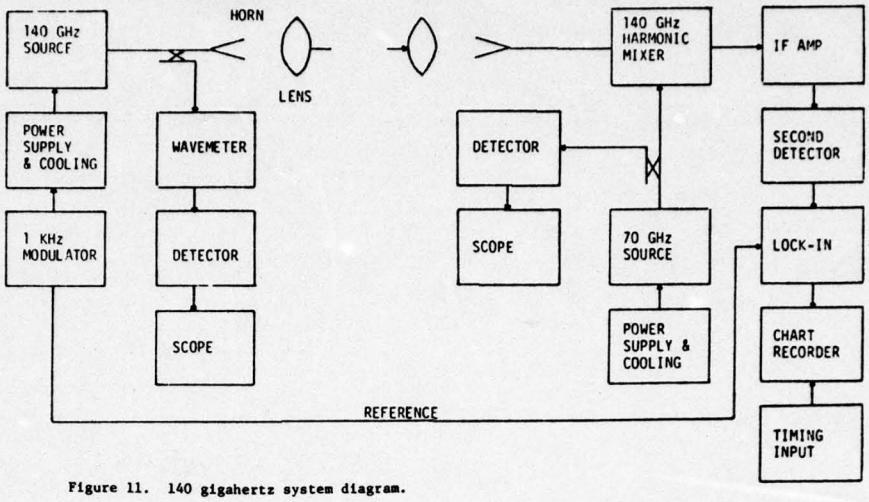

Figure 11. 140 gigahertz system diagram.

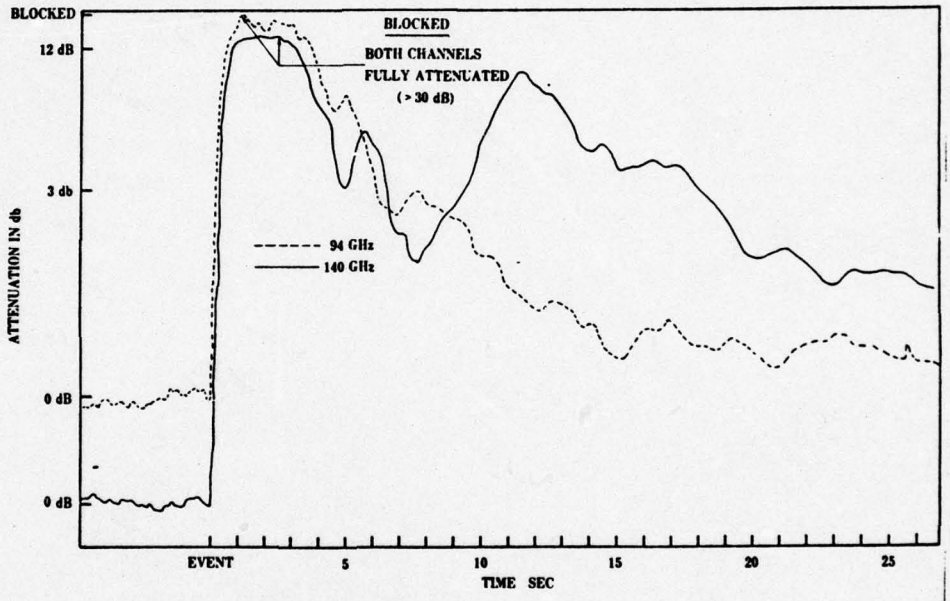

Figure 12. Measurements made during event C - 1, chart speed 1.25 cm/sec., time constant zero.

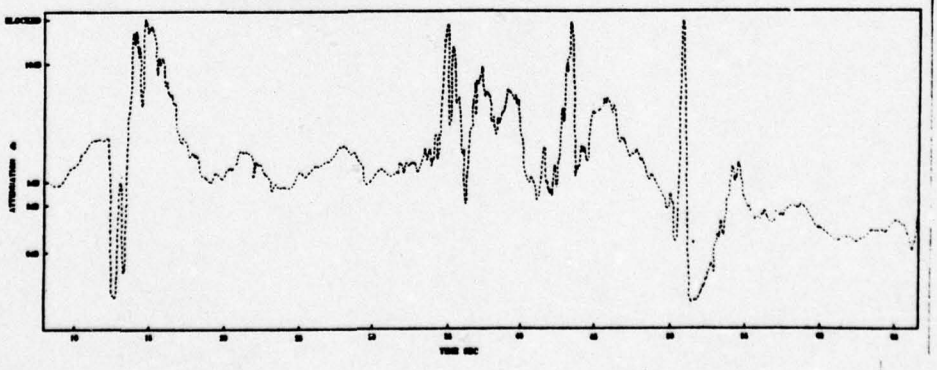

Figure 13. Event F - 2 of 12 October 1978. Three firings of four 155 - mm howitzers at 12 to 45 seconds. The spike at 51 seconds is the result of a late round from the group at 43.2 seconds. Chart speed was 1.25 cm/sec and time constant 40 msec.

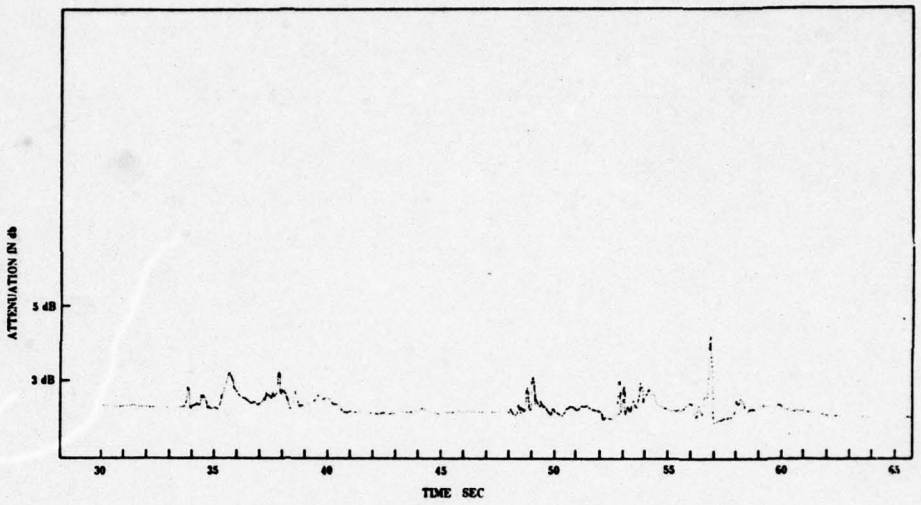

Figure 14: Measurement of attenuation made during event F - 3 of 12 October 1978. Chart speed 1.25 cm/sec, time constant 40 msec.

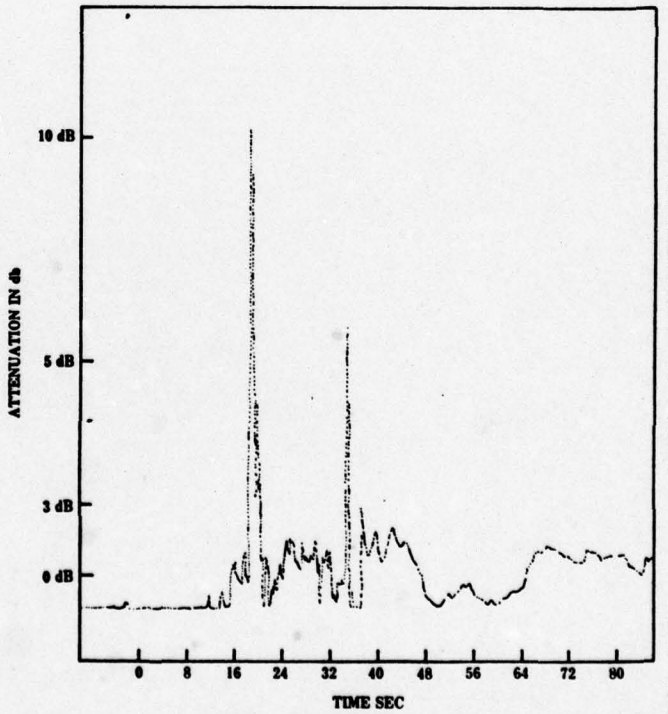

Figure 15. Attenuation measurement made at 94 GHz during event F - 5 of 13 October 1978. Chart speed 15 cm/min, time constant 40 msec.

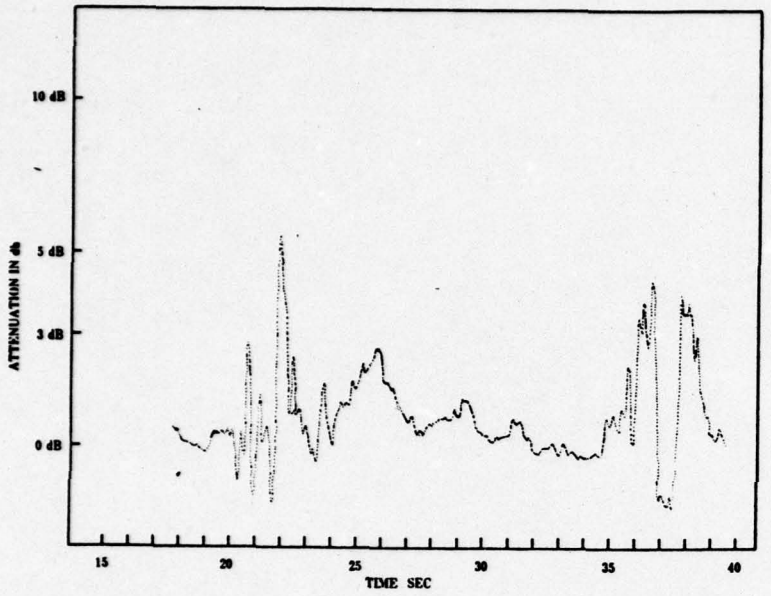

Figure 16. Attenuation measurements made at 94 GHz during event F - 7 of 13 October, 1978. Chart speed = 1.25 cm/sec, time constant = 40 msec.

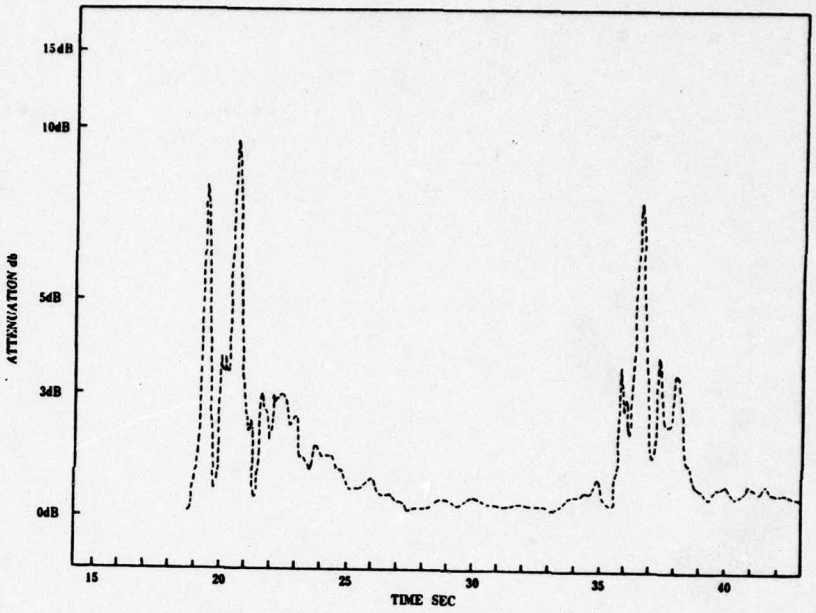

Figure 17. Attenuation measurements made at 94 GHz during event F - 7 of 13 October 1978. Chart speed 1.25 cm/sec, time constant 40 msec.

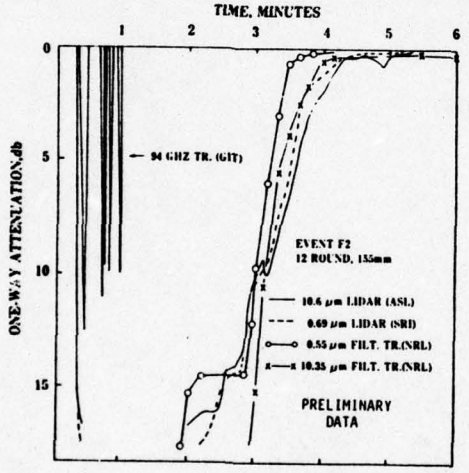

Figure 18. Intercomparison of attenuation at several wavelengths over the 2 km path for event F - 2.

APPENDIX III

Paper Presented To:

23rd Annual SPIE International
Technical Symposium

"Military Systems Applications at
Near Millimeter Wavelengths"

Military systems applications at near-millimeter wavelengths

J. J. Gallagher, R. W. McMillan and R. G. Shackelford

Engineering Experiment Station, Georgia Institute of Technology
Atlanta, Georgia 30332

Abstract

The near-millimeter wavelength region (3.2mm - 0.3mm) is being investigated for military systems applications during adverse weather and in the presence of smokes, dust and other particulate clouds. The use of near-millimeter wavelengths (NMMW) has advantages and disadvantages relative to the use of the infrared and microwave regions. The atmosphere is a dominant factor in determining the operation of military systems in the NMMW region. Systems currently under consideration for NMMW applications include beam rider and command guidance, missile plume detectors, low-angle tracking radars, terminal homing systems, target acquisition radars, fuze systems, quasi-imaging radars and hybrid (IR/NMMW) systems. Recent NMMW technological developments (e. g., sources, receivers, components, phenomenology and measurements) have been advancing at a rapid pace to meet system needs.

Introduction

Weapon guidance systems operating in the visible/infrared spectral regions have been successfully developed for tactical use over a broad spectrum of engagement scenarios. These include direct systems employing beam riders, command guidance, semi-active and active guidance modes which have demonstrated effective operation in clear weather, but are inoperable in certain severe atmospheric conditions and in the presence of smokes, dust and other particulate clouds. Since molecular absorption in the atmosphere is low over broad spectral windows throughout the visible/infrared, the primary attenuation mode is Mie scattering by water droplets in haze and fog, and by particulates in smokes and other aerosols.

On the other hand, the near-millimeter wavelength region is affected less by adverse weather, smokes, and aerosols than the visible/IR wavelength regions. Rain attenuation of NMM wavelength radiation is comparable to rain attenuation in the IR region. Because of its improved transmission under adverse environmental conditions, near-millimeter wavelengths are being considered for military applications. The NMMW spectral region will not prove to be an ideal operational region for all systems applications, but will, in several cases, provide a compromise adverse weather capability for limited range applications with resolution better than that of the microwave region.

In recent years, millimeter and near-millimeter wave systems applications have been the subjects of workshops[1], reports[2] and study panels[3]. This paper will draw upon material presented in these references, with the majority of information originating from the Harry Diamond Laboratories study[3]. A primary purpose of many of these investigations has been the identification of NMMW systems technology requirements, some of which will be briefly discussed following a summary of potential applications.

Advantages and disadvantages of NMMW region

The near-millimeter wavelength region has usually been dismissed in the past as a region of high attenuation, relative to the microwave region, and as a region of poor angular resolution relative to the visible/IR wavelength regions. However, several factors enter into the evaluation of the wavelength region which is chosen for operation of a particular system during adverse weather. It will be seen in the next section that transmission in adverse weather improves considerably in going from visible/IR wavelengths to NMM/MM wavelengths, and further improves at centimeter wavelengths. On the basis of this comparison, it would appear that centimeter or longer wavelengths would be the most appropriate for systems operation in adverse weather. Moreover, it has been shown that transmission through smokes and aerosols also follows a pattern of decreasing with increasing wavelength. Aimpoint accuracy requirements, however, tend to eliminate the centimeter wavelength region on the basis of a number of practical considerations. For example, the required accuracy for target tracking or target designation usually falls within the range of 0.1 to 0.5 mrad resulting in antenna dimensions of about 0.5 to 1 m for millimeter wavelengths and 5 to 10 meters for centimeter wavelengths. This consideration alone rules out a centimeter wavelength system for applications where the weapon system platform would be vehicle- or helicopter-mounted. Analysis of NMMW systems requires then that several factors be weighed in determining their potential in currently conceived tactical applications. Tables 1 - 4 list advantages and disadvantages of the NMMW spectral region relative to microwave and

infrared wavelengths. Some of the listed advantages might be questioned; thus, whereas the best of RF and optical techniques can be combined at NMM wavelengths, this can also be considered a necessity because of the nature of the spectral region. On the other hand, disadvantages such as component deficiencies and lack of data will be reduced or removed as work progresses at NMM wavelengths.

Whereas several of the NMMW disadvantages can be expected to diminish, the limiting factor for systems applications is the atmospheric effect, which cannot be avoided. The factor $e^{-\alpha R}$, where α is the atmospheric attenuation and R is the weapon-target range, is present in all propagation expressions. In the analysis and discussions of NMMW systems, their performance is dominated by their capability to operate under various atmospheric conditions. Since the major role for NMMW tactical systems will be during inclement weather or in the presence of smoke, the characteristics of a NMMW system, when such conditions prevail, are extremely important.

Table 1. Advantages for NMMW Region Relative to Microwave Region

1. Greater Resolution
2. Smaller Beam Angle θ_B for Given Antenna Diameter, D, and Conversely Smaller D for Given θ_B
3. Reduced Multipath Potentially Improved Low-Angle Tracking
4. Low Off-axis Detectability Providing High Security
5. Covertness Due to Exponential Fall-off With Range in High Attenuation Regions
6. Tracking Through Plumes Improved Over Microwave Systems
7. Smaller Components Allowing More Compact On-board Missile Systems
8. Clutter More Diffuse, Doppler Shift is Greater, Glint Should be Less
9. Integration of Hybrid IR/NMMW Systems Possible
10. Countermeasures More Difficult

Table 2. Advantages for NMMW Region Relative to Optical Region

1. Improved Transmission in Smoke and Fog, Providing Better Low Visibility Operation
2. Harder to Jam; More Covert
3. Improved Eye Safety
4. Better Coherent Receiver Techniques
5. Source Stabilization More Easily Performed
6. Potentially Lower Cost
7. Reduced Background
8. Both RF and Optical Technology Applicable

Table 3. Disadvantages for NMMW Region Relative to Microwave Region

1. Poor Heavy Rain Transmission
2. Atmospheric (clear) Absorption is Higher
3. Larger Rain Backscatter
4. Current Receiver Noise Figures are Poorer
5. Higher Precision Manufacturing Required
6. Solid State Source Efficiencies Fall as Frequency Squared
7. Poorer Source Stability
8. Inferior Waveguide Power Handling Capability
9. Higher Cost for NMMW Systems

Table 4. Disadvantages for NMMW Region Relative to Optical Region

1. Lower Resolution
2. Higher Glint
3. Lack of Relevant Data
4. Video Detection Less Sensitive
5. Component Technology Currently Worse
6. NMMW Laser Sources Less Efficient
7. Solid State and Tube Sources Chirped, Less Monochromatic Than Optical Lasers
8. Components Currently Larger and Heavier

Atmospheric effects

Whereas the NMMW region offers an advantage over optical systems during adverse weather, clear weather NMMW propagation suffers greater attenuation than experienced in the IR/visible region, and is, in addition, for most systems restricted to spectral windows. The NMMW region has strong O_2 and H_2O absorption lines with water the major absorber. Between these broad lines lie the transmission windows. Figure 1 shows the horizontal attenuation across the NMMW region from 100 GHz to 1000 GHz at sea level and 4 km altitude[4]. Also shown is the weak O_2 absorption at sea level. Because of the strong absorption at the

short wavelength end of this spectral region, tactical ground-to-ground or ground-to-air applications are confined to the longer wavelength windows which are centered about the following wavelengths:

Wavelength (mm)	Horizontal Attenuation (dB/km)	Zenith Attenuation (dB)
3	.03	1.25
2.1	.05	0.91
1.3	1.75	2.1
0.88	9.0	9.9
0.72	17	22

Included in this listing are approximate horizontal attenuation (dB/km) for 5.91 g/m^3 of H_2O at sea level and the zenith attenuation (dB) for 7.5 g/m^3 of H_2O at sea level. A more comprehensive indication of the horizontal attenuation across the electromagnetic spectrum (3 cm - 0.3 μm) is given in Figure 2. A clear air curve for H_2O density of

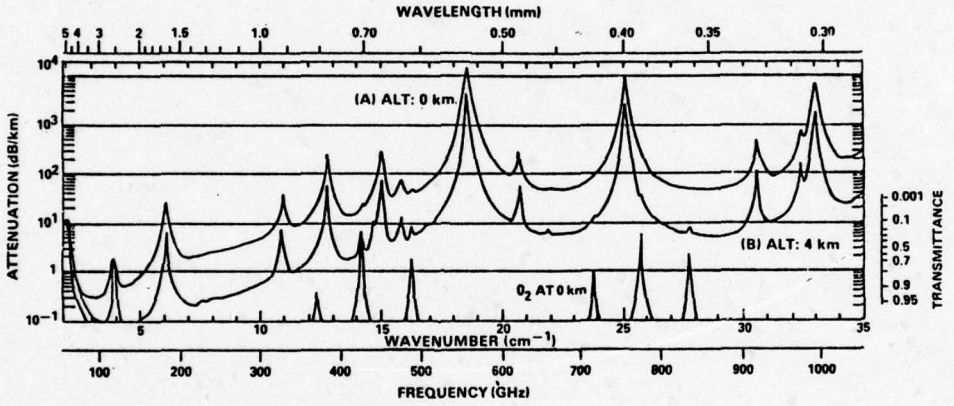

Figure 1. Spectral plots of the attenuation by the (1962) U.S. Standard Atmosphere at sea level and 4 km altitude. The water vapor density is 5.91 g/m^3 at sea level and 1.10 g/m^3 at 4 km altitude. The lower curve represents O_2 only at sea level. For comparison, the attenuation for this same model atmosphere is approximately 0.2 dB/km in the 10 micrometer window and less than 0.1 dB/km near 3.8 micrometers[4].

7.5 g/m^3 at 20°C shows the high attenuation in the submillimeter region surrounded by the low microwave and IR/visible attenuation. From the fog and rain curves of Figure 2, the

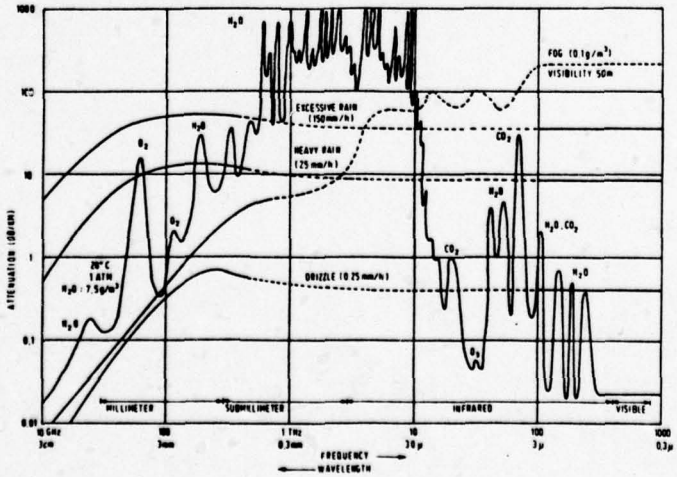

Figure 2. Attenuation by atmospheric gases, rain and fog[5].

advantage of NMMW systems during heavy fog and the comparable NMMW and IR attenuation during rain are demonstrated. A similar figure[6], Figure 3, shown increasing attenuation for clouds with decreasing wavelength, indicating an advantage for satellite or aircraft-to-ground sys-

tems applications. Near millimeter wave attenuation by aerosols is highly dependent on the

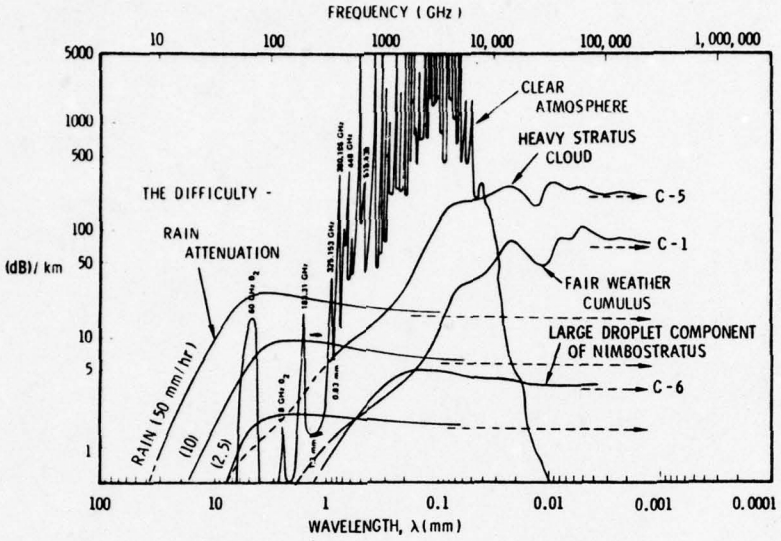

Figure 3. Summary of sea-level atmospheric attenuation[6].

type of aerosol and its particle size distribution and concentration. Table 5 shows the size range and concentration of water droplets in rain, fog and clouds. It can be seen from this table that the larger size range of rain droplets (7-700 μm) would cause significant scattering losses at near millimeter wavelengths were its concentration not extremely low compared to the concentration of water droplets in fogs and clouds. For both rain and fog, the attenuation is an almost linear function of bulk water density with the frequency dependence for attenuation in rain being negligible over the NMM spectral region from 94 to 340 GHz.

Table 5. Comparative Water Droplet Size and Density For Rain, Fog, and Clouds [8, 9, 10]

Rain				
	Light (r = 1 mm/hr)	Moderate (r = 4 mm/hr)	Heavy (r = 25 mm/hr)	Cloudburst (r = 100 mm/hr)
Size Range (μm)	7 - 100	10 - 300	10 - 500	50 - 700
Droplet Density (m^{-3})	350	500	700	1,250
Water Density (g/m^3)	0.04	0.17	1.0	4.2

Fog		
	Thin (vis. ~ 300 m)	Thick (vis. ~ 50 m)
Size Range (μm)	< 0.1	0.02 - 0.2
Droplet Density (m^{-3})	2×10^{10}	1.3×10^{11}
Water Density (g/m^3)	0.023	0.35

Clouds				
	Cumulonimbus	Cumulus Congestus	Fair Weather Cumulus	Strato Cumulus
Size Range (μm)	-	8 - 12	3 - 5	2 - 4
Droplet Density (m^{-3})	-	-	1.6×10^8	3×10^8
Water Density (g/m^3)	6.0	2.5	0.5	0.2

For aerosols resulting from smokes, dust or other battlefield-generated debris, the attenuation is primarily due to scattering, and secondarily to absorption. Preliminary indications[7] are that propagation through existing screening smokes is very high, and that the development of effective smokes for the NMMW region is questionable because of the difficulties involved with generating and dispensing smokes with the appropriate particle size distribution and settling rate. Attenuation of millimeter radiation by ground ex-

plosions of munitions has been shown to be relatively high for short periods of time[7]. Although the attenuation cleared much faster for NMM waves than for the IR/optical bands, nevertheless, loss of NMMW track or acquisition of a target could occur during a barrage or critically placed explosion so that these effects must be considered in greater detail in the future.

It is important at this point to demonstrate millimeter wave propagation under conditions of high absolute humidity and high bulk water content, since these are the conditions under which all military systems are expected to operate. Examples are given for the three cases: clear weather (high absolute humidity), rain and fog.

Clear weather

In high visibility conditions with a lack of precipitation and fog, the attenuation of near millimeter radiation in dB/km is directly proportional to absolute humidity. This linear relationship is shown in Figure 4 on a plot of temperature-humidity data which was abstracted from a psychrometric chart. Table 6 shows the two-way path loss for a range of 3 km at frequencies of 94, 140 and 220 GHz for various atmospheric conditions. Note that the attenuation of 220 GHz radiation is very high for warm, humid conditions although the total path loss is only 18 dB (3 dB/km) for the standard atmosphere (T = 300°K, ρ = 7.5 g/m^3).

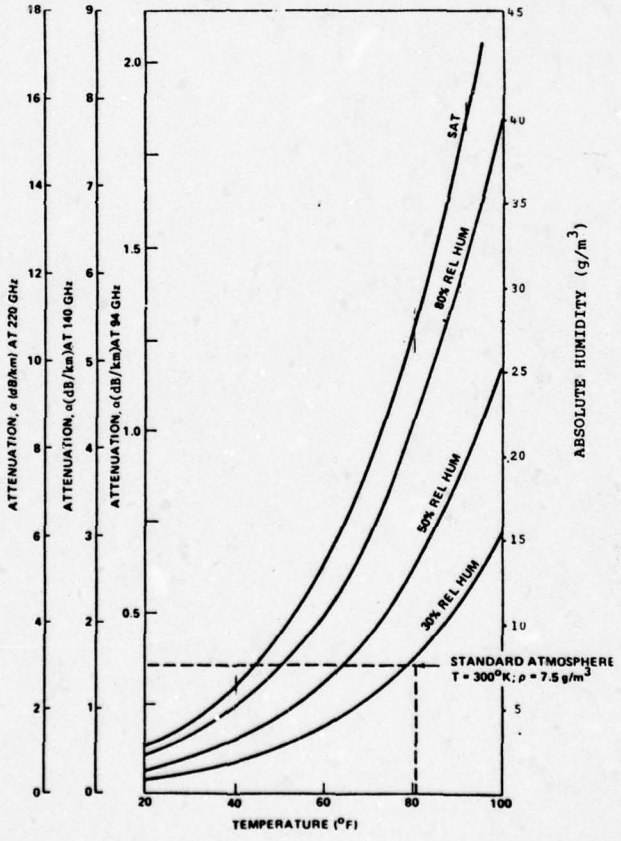

Figure 4. Atmospheric absorption by water vapor.

Table 6. Two-Way Path Loss In dB For Atmospheric Attenuation Over A Range of 3 km

Frequency (GHz)	Relative Humidity =	T = 90°F			T = 65°F			T = 40°F		
		30%	50%	80%	30%	50%	80%	30%	50%	80%
94		3.1	5.2	8.4	1.4	1.9	3.0	0.5	0.9	1.4
140		13.2	21.9	35.4	5.7	9.3	15.0	2.7	3.3	6.2
220		26.4	43.8	70.8	11.4	18.6	30.0	4.5	6.5	12.3

The impact of these attenuation figures on system design can be shown by solving the radar equation for a typical set of system parameters; the radar range equation is of the form

$$S/N = \frac{P_p \tau G^2 \lambda^2 \sigma_T}{(4\pi)^3 R^4 K T N_f L_T} \qquad (1)$$

where P_p = peak power of the transmitter; τ = pulse width of the transmitter (it has been assumed that the receiver bandwidth = $1/\tau$); G = gain of the transmitting/receiving antenna; λ = free space wavelength; σ_T = radar cross section of the target; R = range to target; K = Boltzmann's constant; N_f = noise figure of the receiver, and L_T = total radar system loss (atmospheric & signal processing + waveguide and components).

Assuming the following parameters:

τ = 200 nsec.; λ = 1.3 mm (230 GHz); G = 47.6 dB (6" aperture with η = 0.5); σ_T = 50 m^2; KT = 4.14 x 10^{-21} (T = 300°K); L_s = signal processing loss = 3 dB; L_w = waveguide and component loss = 8 dB; N_f = 12 dB.

we may write

$$S/N(dB) = P_T(dBW) - 40 \log R(km) - 2\alpha(dB/km)R(km) + 15.2$$

Figures 5 and 6 show S/N vs R for different values of P_T for atmospheric conditions of T = 27°C and ρ = 7.5 g/m^3 (standard atmosphere) and T = 30°C and ρ = 28 g/m^3 (relative humidity ≈ 80%). For these two cases, Table 7 shows the peak power versus range required for S/N = 14 dB (P_d = 0.9, P_{fa} = 10^{-7}). Note that for large α, the S/N vs R curves are very steep, and only small changes in range occur for large changes in P_T at a given S/N. With a maximum peak power of 10 kW, for example, the high visibility range will be limited to about 1.5 km on a warm humid day, and to about 3 km on a warm dry day. These calculations are for single pulse transmission only.

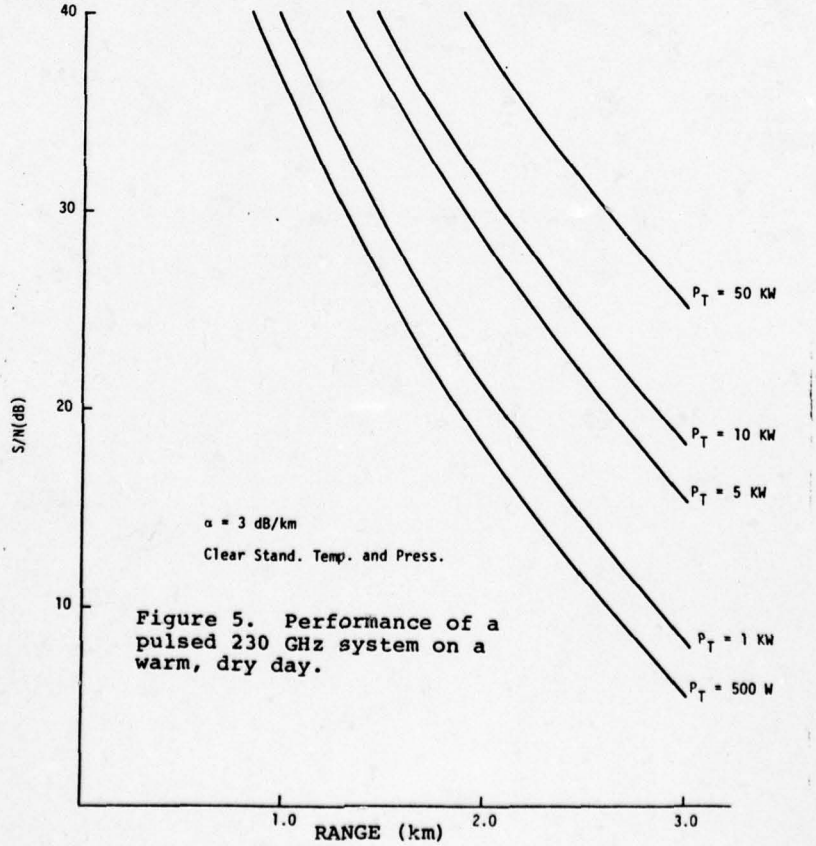

Figure 5. Performance of a pulsed 230 GHz system on a warm, dry day.

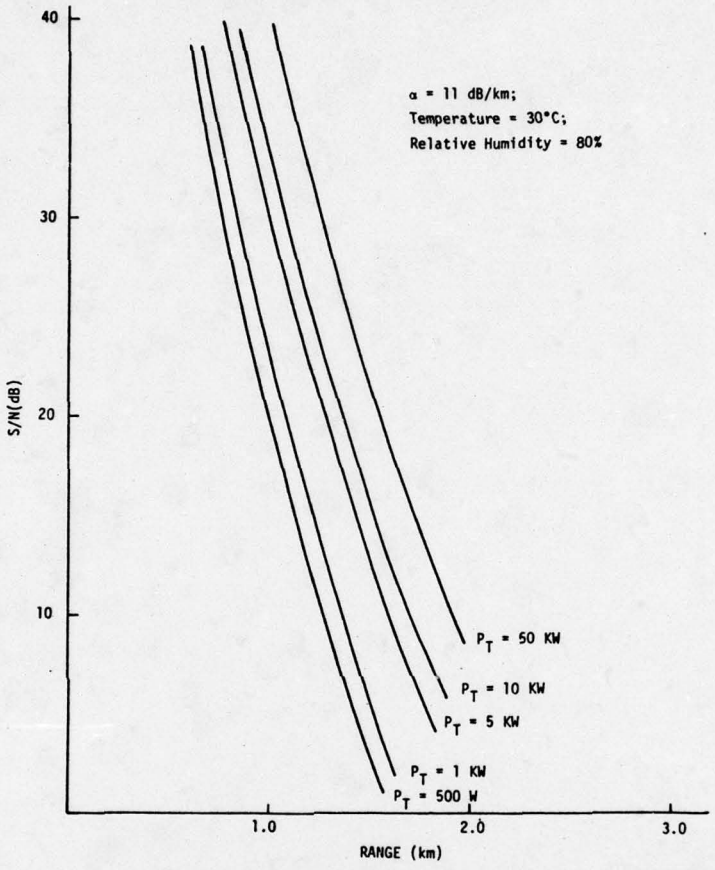

Figure 6. Performance of a 230 GHz pulsed system on a warm, humid day.

Table 7. Required Power To Achieve S/N = 14 dB

Range (km)	Warm, Dry T = 27°C, ρ = 7.5 g/m^3 P_T(KW)	Warm, Humid T = 30°C, ρ = 28.0 g/m^3 P_T(KW)
1.0		0.1
1.25		1.0
1.5		7.2
1.75		47.0
2.0	0.2	284.5
2.25	0.4	
2.5	0.9	
2.75	1.8	
3.0	3.6	

Although the performance of a system operating in the 230 GHz window degrades rapidly in warm humid weather, in many parts of the world these conditions are present for only a small percentage of the time. An example is the climatological conditions of Western Europe. Figure 7 shows the attenuation for three near-millimeter frequencies based on the mean maximum daily temperature and relative humidity for Bayreuth, West Germany. These data predict that the mean attenuation during the summer months will be less than 7 dB/km, and for this figure, a range of 2.0 km would be possible with a 10 kW pulse source.

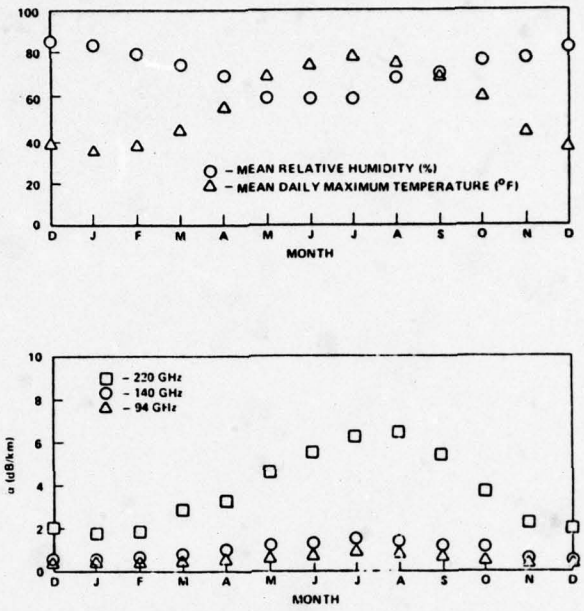

Figure 7. Millimeter wave atmospheric absorption by water vapor - Bayreuth, West Germany.

Rain. Although differences exist in predicted rain attenuation for the NMMW region[11], most models predict the following relationships:

$$\alpha(\text{dB/km}) = Ar^B, \tag{2}$$

where A and B are constants for the frequency region 94 - 340 GHz, and r is the rain rate in millimeters per hour. Based on the available data, the relation

$$\alpha(\text{dB/km}) = r^{0.85} \tag{3}$$

provides a reasonably close fit throughout the NMMW spectrum. As might be expected, a warm rainy day will be a problem for a system at 220 GHz because of strong absorption by both water vapor and bulk water. For example at T = 26.7°C (80°F), and r = 4 mm/hr. (a moderate rain rate), the attenuation is 11 dB/km (water vapor) plus 3 dB/km (rain) or 14 dB/km total. Figure 8 shows the S/N versus range at three power levels, and again it is evident that for a given value of S/N, large increases in power result in small increases in range. For this atmospheric condition, a peak power level of about 50 kW would be required for a range of 1.5 km at S/N = 14 dB whereas a range of about 1.2 km would be possible at the same value of S/N with only 5 kW peak power. An order of magnitude increase in power only results in about 0.3 km increase in range for this condition.

Fog. Attenuation of NMMW radiation by fog is also dominated by bulk water absorption, although a slight frequency dependence is also present. A good fit to available fog attenuation data is provided by the expression

$$\alpha(\text{dB/km}) = 0.035\ \rho(\text{g/m}^3)\ f^{1.08}(\text{GHz}) \tag{4}$$

This relationship along with the optical visibility is shown in Figure 9. For a 30 meter visibility radiation fog, with liquid water content of 0.75 g/m^3, the attenuation by water absorption at 230 GHz is approximately 9 dB/km. As shown in Figure 7, the mean maximum daily temperature of Bayreuth, West Germany during the winter months (the season of greatest incidence of fog) is about 0-4°C; therefore a reasonable fog scenario is 30-100 m visibility with temperature 0-4°C, for which the attenuation at 230 GHz would be approximately 4 dB/km to 11.5 dB/km. These conditions have been bracketed by the calculations presented in Figures 5 and 8. It is significant to point out that a 100 m visibility fog at T = 4°C (40°F) results in an attenuation of only 4.5 dB/km at 230 GHz compared with about 50 dB/km in the 8-12 μm band and about 150 dB/km at a wavelength of 0.6 μm.

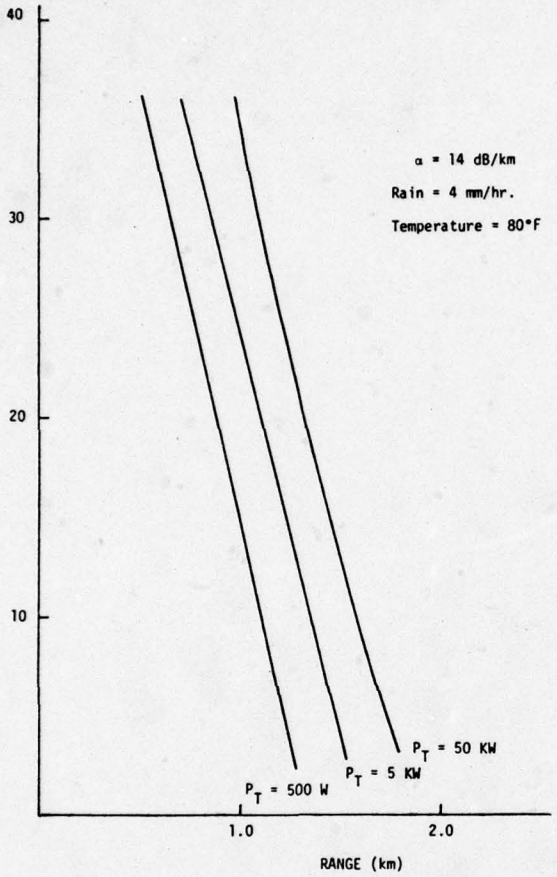

Figure 8. Performance of 230 GHz pulsed system in rain.

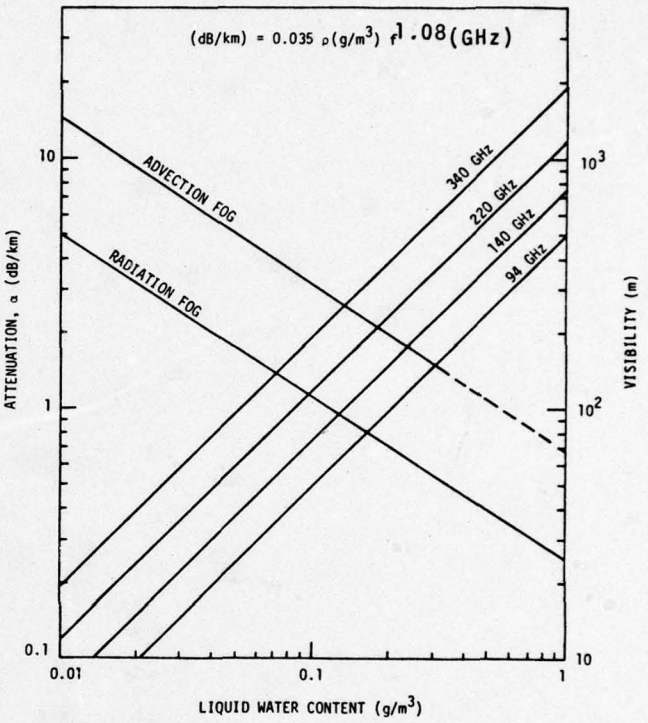

Figure 9. Millimeter wave attenuation by fog.

A summary of atmospheric propagation data, convenient for system calculations, is given in Table 8. The majority of information presented thus far has dealt with atmospheric effects appropriate to radar or communication applications. An equally important consideration is the influence of the atmosphere and environment on radiometric signals. When observing a target in its surroundings, it is important to know the brightness temperature contrast between target and other objects. This contrast is a function of frequency, the atmosphere, and target and background characteristics (reflectivity, emissivity, etc.). The antenna temperature of a radiometer looking downward from altitude h at an angle θ to the vertical is given by

$$T_B = \int_h^0 T(z)\exp[-\tau(h,z,\theta)]\alpha(z)\sec\theta dz + R\exp[-\tau(o,h,\theta)]\int_h^0 T(z)\exp[-\tau(z,o,\theta)]\alpha(z)\sec\theta dz + (1-R)T_E\exp[-\tau(o,h,\theta)]$$

where T_E is the temperature of the earth- or ground-based target and $T(z)$ is the temperature of a stratum of atmosphere of thickness dz located at altitude Z. The terms of the form $\tau(Z_1, Z_2, \theta)$ are the optical depths between altitudes Z_1 and Z_2 at angle θ, and R is the reflectivity of the earth or target. The optical depths τ are given by

Table 8. Summary Of Propagation Data

Attenuation, α (dB/km)
Water Density, ρ (g/m^3)

	α Clear Rel. Humidity = 100%		α Fog	α Fog						α Rain			α Cloud	
			Radiative Fog				Advection Fog				mm/hr		Fair	
λ (μm)	T = 32°F ρ = 4.8	68°F 17.4	R_v = 400m ρ = 0.014	200 0.038	100 0.11	30 0.71	400 0.063	200 0.18	100 0.4	1	4	10	Weather Cum.	Nimbo-Strat.
1				80		500							95	570
4													120	640
10.6	0.3	1.2	7	20	58	373	17	63	140	1	2.6	6	50	500
337	50	185	0.6	1.5	4.3	28	2.5	7.1	15.8	1	3	7	3	20
724	10	37	0.3	0.9	2.6	17	1.0	4.3	9.6	1	3	7	2	7
880	7	24	0.3	0.7	2.0	14	1.2	3.5	7.9	1	3	7	1.5	6
1300	2	6	0.2	0.5	1.4	9	0.8	2.3	5.1	1	3	7	0.8	4
2300	1	3	0.1	0.2	0.6	4	0.4	1.0	2.2	1	3	8		2
3200	0.2	0.9	0.1	0.2	0.5	3.2	0.3	0.8	2	1	3	8		1.5

Notes: (1) for α_{CLEAR} at other Rel. Hum., scale down from 100% given

(2) for a fog situation, $\alpha_{TOTAL} = \alpha_{CLEAR}$ (RH = 100%) + α_F (likewise for clouds)

(3) for a rain situation, $\alpha_{TOTAL} = \alpha_{CLEAR}$ (RH = 100%) + α_R

$$\tau(Z_1, Z_2, \theta) = \int_{Z_1}^{Z_2} \alpha(Z) \sec \theta dZ \qquad (6)$$

so that the first term of Equation (5) is the contribution of the intervening atmosphere between the radiometer and target, the second term represents atmospheric emission reflected from the target to the radiometer, and the third term is the target's emission attenuated by the atmosphere between the radiometer and target. The target or earth background reflectivity is given by R, the target (earth) temperature is T_E and the atmospheric attenuation is $\alpha(Z,\nu)$. It is seen from these relations that not only atmospheric absorption by O_2 and H_2O is important, but hydrometeorite absorption and scattering and atmospheric thermal emission are also determining factors for the radiometric antenna temperature, which is reduced further in value when the target fill factor for the antenna is less than one.

Preissner[12] has shown the brightness temperature contrast for different weather conditions and different materials for the microwave through NMMW spectral region. Figure 10 demonstrates the brightness temperature contrast between vegetation and concrete for three different altitudes for a clear standard atmosphere (ρ_{H_2O} = 7.5 g/m^3, T = 20° C and P = 760 mmHg at sea level). At all altitudes given, a detectable brightness temperature contrast exists, except possibly at 230 GHz for 3 km and 8 km, where the temperature contrast is on the order of 3-5° K and the minimum detectable temperature is approximately 0.5-3° K for a 1 GHz bandwidth and a 10 msec time constant. Figure 11 shows the brightness temperature contrast (concrete and vegetation) for a radiometer at 3 km altitude for several atmospheric conditions. Rain severely degrades NMMW radiometric response and fog of visibility of 100 m or less results in considerable loss of contrast. A more significant indication of radiometric capability to detect a military target is the brightness temperature contrast for metal relative to vegetation. Figures 12a and 12b show contrasts for metal, water and concrete relative to vegetation. For metal, detectable contrasts are observed for all conditions except the 25 mm/hr rain. It must be emphasized, however, that, for metal, reflectivity of 1 has been used and no fill factor reduction has been employed. Both conditions are unlikely. Systems applications require further consider-

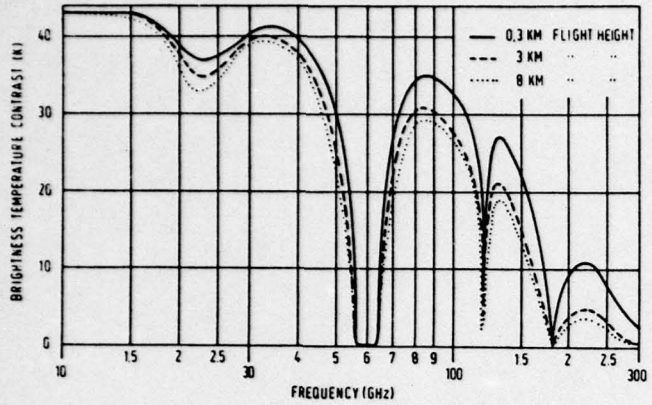

Figure 10. Brightness temperature contrast between vegetation and concrete for three different heights[12].

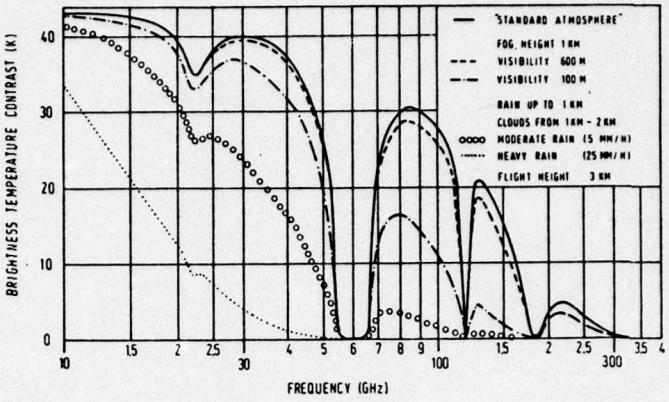

Figure 11. Brightness temperature contrast between vegetation and concrete for different weather conditions[12].

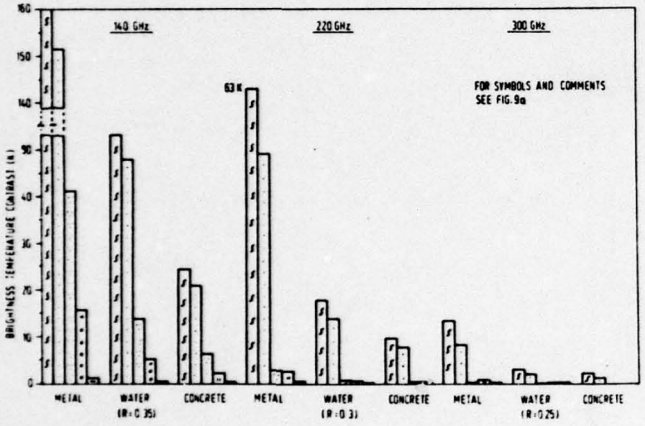

Figure 12a. Brightness temperature contrast for different objects, weather conditions and frequencies (11 GHz, 140 GHz, 90 GHz)[12].

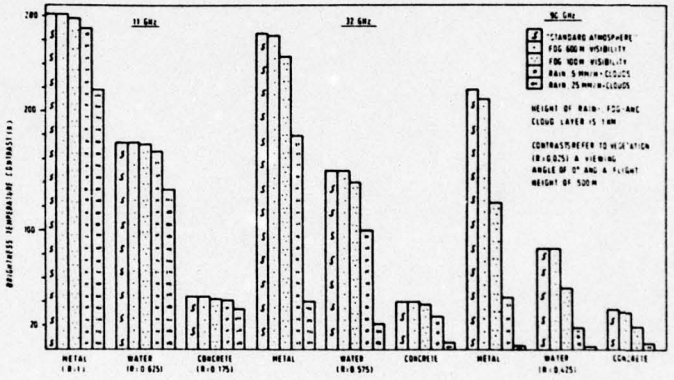

Figure 12b. Brightness temperature contrast for different objects, weather conditions and frequencies (140 GHz, 220 GHz, 300 GHz)[12].

ation of these effects with inclusion of antenna pattern and fill factor effects.

Very little data exist for atmospheric turbulence in the NMMW region; fluctuation of intensity and signal angle of arrival for NMMW systems have been studied by Armand et al.[13] and by Snider, Wiltse and McMillan[14]. Based on the approach first proposed by Armand, the peak-to-peak intensity fluctuations expected for a 230 GHz system under near standard conditions were calculated to be 1.16 dB, and the corresponding angle-of-arrival fluctuations were determined to be 0.3 mrad. In practice, observed intensity fluctuations at lower frequencies have occasionally been observed to be much larger, and little data are available for the angular fluctuations. Much work needs to be done before the effects of turbulence on NMMW systems have understood, but the meager results available to date indicate that it gives system degradation of a magnitude which must be considered.

The approximations discussed thus far demonstrate some of the atmospheric effects to be considered in systems trade-offs between the NMMW and IR/visible regions but do, in no way, describe the complexity that could occur at NMM wavelengths. Thus, when the limited experimental data for H_2O are compared with existing theories, the measured values in the window regions invariably exceed theoretical values. When measured values are compared with the monomer spectrum calculated with the Van Vleck-Weisskopf[15] or Gross[16] lineshape, the inadequacy of the theory is evident from Figure 13 in which the dashed curve B represents an empirical "continuum" absorption which must be added to bring the theoretical results into coincidence with the experimental results[4]. The empirical correction term has been given in the form[17]:

$$\Delta \alpha_\nu = 4.69 \times 10^{-6} \rho \left(\frac{300}{T}\right)^{2.1} \left(\frac{P}{1000}\right) \nu^2 \left(\frac{dB}{km}\right) \qquad (7)$$

where ρ is the water density (g/m^3), T is the atmospheric temperature, ^oK, P is the pressure and ν the frequency. The discrepancy between measured and calculated water-vapor absorption closely follows this empirical correction term throughout the NMMW region. Various causes have been postulated for this excess or anomalous absorption, but, thus far, the source is not understood. Great anomalies have been observed in high humidity, cold conditions and in fog[18]. Further experimentation is needed in this area of atmospheric effects.

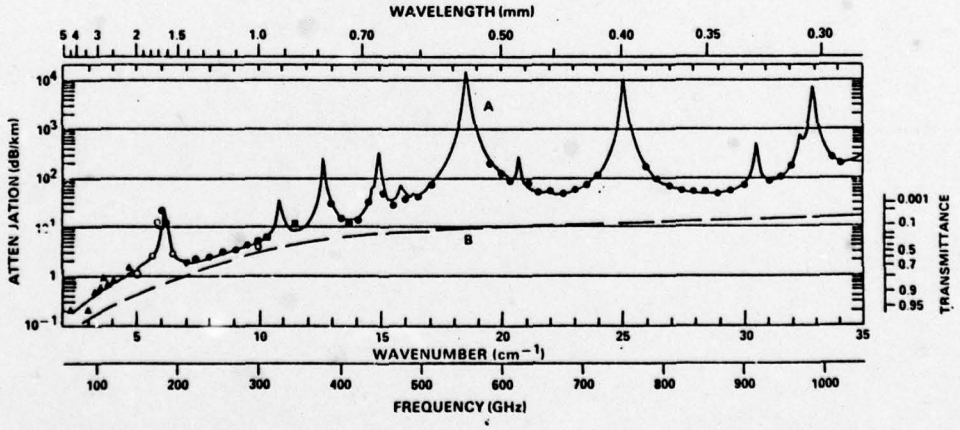

Figure 13. Spectral plots of the attenuation by atmospheric H_2O at sea level. Curve A represents a combination of theoretical and experimental results for an H_2O density of 5.91 g/m^3. At a fixed temperature and 1 atm total pressure, the attenuation is approximately proportional to the H_2O density. Curve B corresponds to an empirical continuum that is added to theoretical results to provide agreement with the experimental results. The transmittance scale on the right-hand side corresponds to a 1 km path[4].

Considerable space has been devoted in this paper to a discussion of atmospheric effects on propagation. However, it is just these effects which are the most important factors in determining the applicability of a particular military system in the NMM wavelength region.

Potential NMMW systems applications

Several NMMW military applications have been investigated in recent years. Of these, some have not shown advantages over the equivalent system operating in another spectral region, whereas some have sufficient promise to warrant initiation of experimental development of prototype systems. Among the potential systems applications which have been studied are the following[1-3]:

1. Beamrider systems
2. Terminal homing
3. Target designation and semi-active homing
4. Command guidance
5. Target surveillance and acquisition
6. Active NMMW quasi-imaging
7. Low angle tracking
8. IFF systems
9. Airborne passive imaging
10. Aircraft detection from satellites
11. Boost phase plume detection
12. Re-entry applications
13. Secure communications
14. Mine detection
15. Obstacle and terrain avoidance
16. Space object identification (SOI)
17. Fuzing
18. Hybrid (IR/NMMW) systems

The details of the investigation of most of these systems can be found in the references, and only a selected system, the NMMW beamrider, and brief statements on others will be discussed in this section.

Beamrider

A beamrider guidance system[19, 20, 21] is defined as a technique for guiding missiles which utilizes a beam directed into space, such that the beam axis forms a line along which it is desired to direct a missile. The missile contains equipment that can sense the direction and magnitude of the error when its path has deviated from the center of the beam, and that can generate guidance error signals which cause the missile to return toward the center of the beam. In principle, a beamrider system can be employed in surface-to-surface, surface-to-air, air-to-air, and air-to-surface roles, although it is potentially more effective against slowly moving targets. The basic elements of a beamrider system are the same for each of the roles but the stringency of the requirements placed on these elements will be determined by the particular applications. For the purposes of interest here, a surface-to-surface anti-armor role has been emphasized as an example of a credible application of NMMW guidance.

In the beamrider concept adopted as an example for this study, the target is acquired and tracked by a precision near millimeter wave (NMMW) radar with a conical scan antenna. The missile is launched toward the target along the conical scanning tracking beam, which is coded to provide information on the position of the missile relative to the scan axis which defines the line-of-sight (LOS) to the target. A receiver in the rear of the missile detects the scanning beam, decodes it to determine its position with respect to the scan axis, and generates the appropriate error signals to keep the missile in the center of the beam. In the conical scan mode, a relatively simple PRF coding scheme can be used to develop the required guidance error signals.

Figure 14 shows the NMMW beamrider guidance concept. The first and second beams are the capture beams which establish line-of-sight (LOS) guidance as quickly as possible. The basic functions of the beamrider system are target acquisition, target track, missile capture and missile guidance.

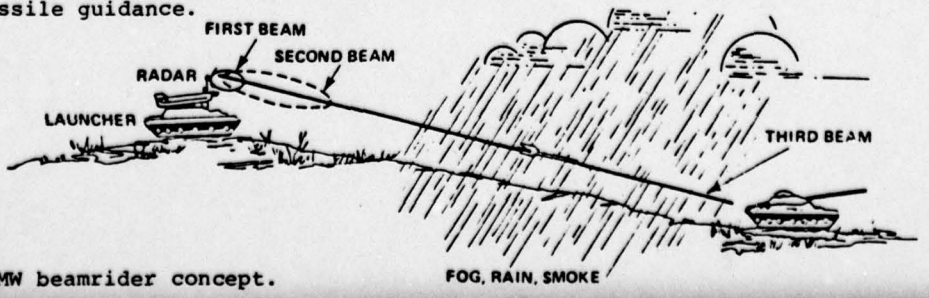

Figure 14. NMMW beamrider concept.

The basic system configuration considered to be most desirable for a ground-to-ground, anti-armor beamrider system requires that the entire system be a self-contained, crew-served and vehicle-mounted package with an antenna aperture diameter less than one meter. The candidate missile would be of the TOW or SHILLELAGH generic class, and would be tube-launched from the tracking/guidance platform. This concept would require an integrated target acquisition capability for performing target handover from a wide-area battlefield surveillance system, and for establishing an autonomous operating capability over a limited battlefield sector. The acquisition capability would of necessity require the development of suitable target recognition criteria based on the near millimeter wave target signature.

Nominal system parameters relating to these requirements have been given as the following[21]:

Operating Range	- Maximum: > 2 km; Minimum: < 0.5 km
Capture Range	- Maximum: $\leq$ 100 m
Weather and Environmental Extremes	- Rain: 4 mm/hr; Fog: 100 m vis. Temperature: 90 - 100°F; Relative Humidity: 80 - 100% Smoke: Battlefield-generated dust and aerosols; tactical screening agents
Acquisition	- Search Sector: 5° x 25°, movable scan sector; Search Time: < 10 sec.
Missile Data Rate	- 50 Hz

In addition to these characteristics, a NMMW system should also satisfy the general requirements of high reliability and maintainability, compatibility with existing equipment, capability for CM hardening, minimum operator interaction and training, rapid fire capability, and high first round probability of kill.

Based on these requirements, system concepts and estimated performance for a NMMW anti-armor beamrider system have been addressed[21]. However, the paucity of essential data for target and terrain reflectivity and atmospheric propagation may result in an altering of the performance calculations when those data become available.

The beamrider concept has been successfully implemented in the infrared, demonstrating good clear weather performance. Currently, there is an enthusiastic interest in the beamrider for the anti-armor application. The U. S. Army Ballistic Research Laboratory (BRL) has successfully carried out a feasibility demonstration of beamrider tracking and guidance at 140 GHz[20], and plans to repeat these experiments at 217 GHz. Efforts have also been initiated at U. S. Army MIRADCOM to define and verify a baseline beamrider missile system for anti-armor applications.

The critical performance parameters of any beamrider system are related to (1) high accuracy centroid tracking of the target, (2) a temporal and spatial beam structure such that the missile guidance is not biased by the terrain effects, and (3) a method of capturing the missile at a range close enough to insure adequate damping of the missile's angular deviations from LOS at the closest tactical range of interest.

The application of beamrider technology is most promising in the guided direct fire anti-tank role with the radar and launcher borne by a land vehicle. The system as presently envisioned requires a relatively large antenna ($\sim$ 0.6 m diameter), a precision tracking mount, and a dual beamwidth antenna configuration to accomplish missile capture. It is not feasible to consider a helicopter-borne weapon system at this time because of the size of the antenna/mount configuration; however, it may be possible to exploit optical scanning techniques which involve stabilization of scan components to obviate the requirement for a large precision tracking mount. The anti-helicopter role could be considered if the target exposure time is adequate to acquire and to accommodate the missile time-of-flight. In the anti-aircraft role the end game maneuverability requirements on the missile would be severe for crossing targets or for targets performing high G maneuvers; however, such a system appears to be feasible.

In considering why a beamrider system should be investigated as the initial concept for NMMW guidance feasibility rather than another scheme, the following factors are influential:

(1) The guidance link is one-way, so that relatively simple video receivers are potentially adequate for the missile link.

(2) Beamrider guidance has been demonstrated at IR and optical wavelengths in operational situations so that it is not necessary to go through a concept demonstration phase.

(3) Target cross section is high because the tracker looks at backscatter rather than at off-axis scatter.

(4) Since only the low cost missile receiver is expended in firing, the cost per round could be significantly less than that for a missile employing an active seeker.
(5) The missile is difficult to jam since the receiver looks back at friendly territory.
(6) It is possible to implement a multiple wavelength system so that wavelength optimization is possible for the acquisition, tracking and guidance functions.
(7) The airframe could be optimized aerodynamically since there is no seeker to complicate the warhead. Complexity of the on-board guidance and control is minimal.

The NMMW beamrider system must perform several functions in sequence, with the capability for continuity or rapid handover from one function to the next. This system must be capable of searching for and acquiring a target over a limited field-of-view (FOV), followed by the target tracking and missile guidance. Handover from the tracking to guidance modes must include a missile capture phase during which the missile is launched toward the target and LOS guidance along the tracking radar beam is established. For simplicity, it is desirable that one system at a single wavelength perform the entire beamrider operation; however, because of the complexity of these multiple operations (target acquisition, tracking, missile capture and guidance), the optimum configuration might require a multi-wavelength system.

Several approaches for implementation of the beamrider system have been investigated[21]. Performance in inclement weather is the most important consideration for a NMMW beamrider. For 94 GHz, 140 GHz and 220 GHz, an example of the transmitter power requirement for target acquisition as a function of range for rain rates of 4 and 16 mm/hr on a warm day is given in Figure 15. The following parameters are used in the calculations for source power:

	94 GHz	140 GHz	220 GHz
λ (m)	3.19×10^{-3}	2.14×10^{-3}	1.36×10^{-3}
G_T (dia. = 0.6 m; η = 0.5)	1.78×10^{5}	3.88×10^{5}	9.60×10^{5}
σ_T (m^2)	30	30	30
L_{RF}	0.5	0.40	0.16
S/N	3.1 (4.9 dB)	6.2 (7.9 dB)	38.9 (15.9 dB)
kTB (B = 10^7 Hz)	4.14×10^{-14}	4.14×10^{-14}	4.14×10^{-14}
N_f (dB)	4	7	15

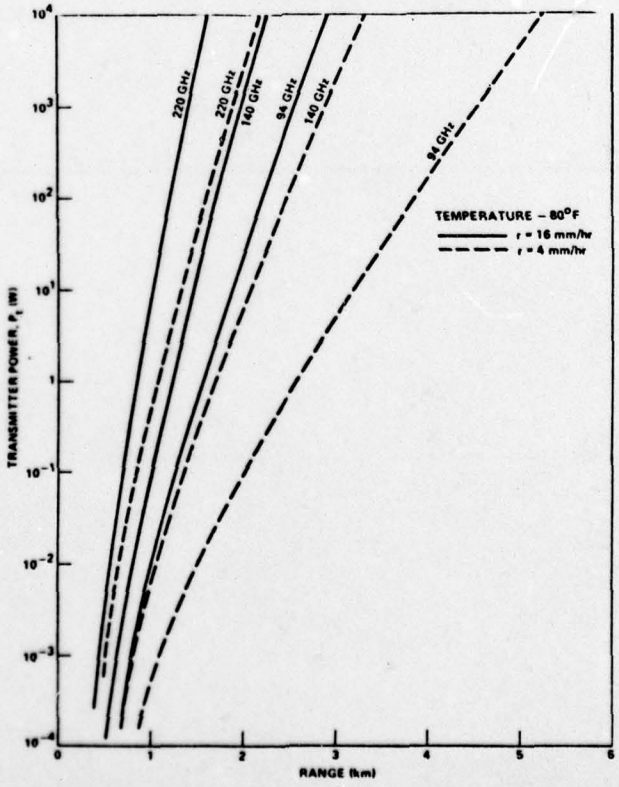

Figure 15. Power required for target acquisition on a warm day with moderate to heavy rain.

Trade-offs between search time, PRF, and antenna beamwidth must be considered in designing a beamrider system. If a separate acquisition system is employed, the required S/N for tracking will be considerably improved by the integration of additional pulses during the tracking interval which is long with respect to the acquisition target dwell time.

The curves of Figure 15 show that only the 94 GHz system is capable of a range of 3 km with a power of 1 kW in moderate rainfall. The transmitter power requirements for missile guidance are not as severe as those required for acquisition and tracking because the guidance link is a one-way path. It has been shown[21] that power levels required for acquisition are more than adequate for guidance.

For a five year projection of system performance, it would seem reasonable to anticipate improved noise figures and decreased RF losses at 140 and 220 GHz. These projections of improved performance are listed below:

Frequency (GHz)	State-of-the-art			5 Year Projection		
	L_{RF}	NEP	N_f	L_{RF}	NEP	N_f
140	4 dB	1.6×10^{-12}	7 dB	3 dB	10^{-12}	6 dB
220	8 dB	5×10^{-12}	15 dB	3 dB	10^{-12}	6 dB

The reason for projecting the same parameters for both frequencies is that quasi-optical components should show very little frequency dependence over the range, and the cutoff frequency of Schottky barrier mixers is presently about 3000 GHz.

Target acquisition, guidance with video detection and tracking have been calculated with the projected parameters. For tracking, it is assumed that the tracking error is

$$\sigma_m \approx \frac{CEP}{\sqrt{3R}} = \frac{0.35}{R(m)} ,$$

and a pulse integration gain of 17 dB is also assumed.

The projected performance levels for acquisition and tracking are shown in Figures 16 and 17 for each of the frequencies and a 1 kW source. Corresponding curves for guidance were not plotted because power adequate for the other two functions is more than adequate for guidance. These curves show some improvement over those of Figure 15; in particular, they show that it is possible to achieve tracking and guidance at a range of 3 km under more stringent conditions than before.

The calculations in the study show that, neglecting angle error due to multipath and glint, 94 GHz is the best frequency for a multifunctional tracking, acquisition and beamrider guidance system using state-of-the-art performance parameters. For a system dominated by multipath effects, either 140 or 220 GHz appears to be the preferred choice for operating frequency; whereas, without the presence of multipath effects, 94 GHz is a better choice for development of first generation millimeter guidance systems. This result is to be expected for performance dominated by propagation effects, since the absorption due to water vapor is much higher at 140 and 220 GHz than at 94 GHz. On the other hand, it would seem that tracking accuracy would favor 140 or 220 GHz in view of the reduced beam divergence at shorter wavelengths. For a conscan tracker, the tracking error due to thermal noise is $\approx \theta_B/\sqrt{S/N}$, and the $\sqrt{S/N}$ decreases faster than θ_B as the wavelength goes to 2.14 mm (140 GHz) and 1.36 mm (220 GHz) due to the increase in mixer noise figure and atmospheric attenuation coefficients at the shorter wavelengths. Even for projections based on extrapolation of available source power and improved performance of quasi-optical components, the 94 GHz window is still slightly preferable in terms of tracking accuracy for a system in which multipath is not a consideration.

On the other hand, if the multipath model adopted is valid, there are indications that 94 GHz will not provide adequate angle tracking error over typical types expected to be encountered in tactical operations in adverse environments. If the trend of these calculations is consistent with projected performance from realistic terrain models, operation at 220 GHz may also be necessary to insure an adequate accuracy for missile impact over the desired clear weather range of 3 km. If this is the case, a reduced low visibility operating range will be incurred. Thus, among the trade-offs to be considered will be that of adequate clear weather operation against maximum range of low visibility operation. A 94 GHz system, for example, might perform reasonably well over a 1.5 - 2 km range interval in a wide range of adverse meteorological and terrain conditions, whereas a 220 GHz system might extend the clear weather operating range to 2.5 - 3 km while restricting the adverse

weather range to < 1.5 km.

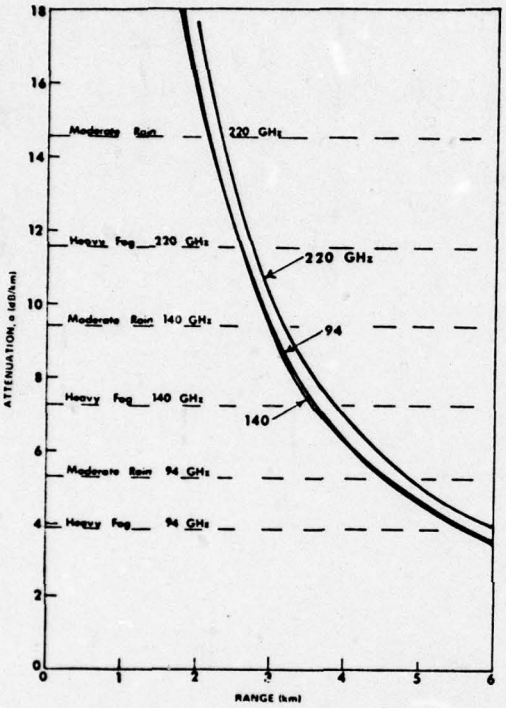

Figure 16. Projected performance levels for acquisition under different weather conditions for a 1 kW source. The conditions are: moderate rain 4 mm/hr, 80°F; heavy fog, 30 m visibility, 40°F.

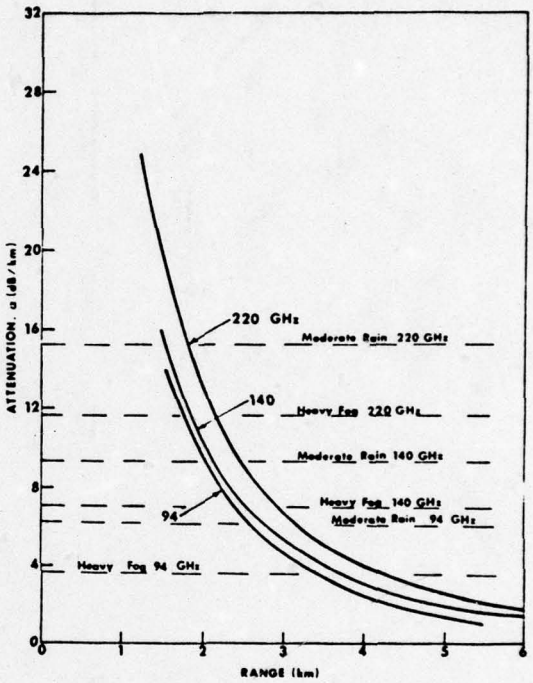

Figure 17. Projected performance levels for tracking under different weather conditions. The conditions are the same as those given in Figure 16.

Preliminary system studies have shown that millimeter guidance systems offer a potentially significant improvement in penetration of adverse environments which limit the visibility of electro-optical guidance systems. Further, there is the potential for improved accuracy with adequate penetration under adverse environmental conditions when compared to guidance systems operating in the microwave frequency band.

The state-of-the-art will currently support the development of operational breadboard beamrider or command guidance systems at 94 or 140 GHz. One such breadboard system has been developed at BRL[20], and tests performed at both BRL and MIRADCOM on tracking and guidance link operational simulations were found to be supportive of this millimeter guidance concept. MIRADCOM is also supporting several contractor-developed millimeter guidance systems which will involve development and testing of both differential guidance and beamrider concepts. As a part of these efforts, the evolutionary development of critical subsystems such as the tracking radar and guidance link will provide a means for performing operational tests to determine multipath effects, measure target signatures, and assess various schemes which have been proposed for missile capture; however, a very significant concern is the development of an appropriate target acquisition concept for an autonomous millimeter guidance system, and this and other critical technology issues are addressed in Table 9.

A basic deficiency in the current millimeter technology base is the lack of measured target, terrain and atmospheric data. Without these data, accurate quantitative estimates of system performance in realistic tactical environments cannot be made with any degree of confidence. Thus, the development of millimeter measurement systems operating in the windows at 94, 140 and 220 GHz is a critical step in establishing their operational limitations in terms of meteorological conditions and reduced visibility situations resulting from smokes and other battlefield-generated aerosols. The acquisition of these data should be a major part of a program to develop millimeter guidance systems.

acquisition, and guidance. Among the systems that have been identified as potential NMMW applications are:

battlefield ground-to-ground target acquisition;
airborne surveillance by RPV radars of land-based targets;
long-range surveillance and target acquisition;
target acquisition for NMMW airborne missile seeker systems;
horizon search radars;
shipboard surveillance radars;
track-while-scan systems for short-range self-defense systems (point defense);
restricted scan target acquisition for missile systems.

A large number of equipment and technique developments are necessary to ascertain the applicability of NMM waves. Techniques for search, recognition and classification have been identified [3] but more detailed investigations are needed to implement these techniques. Greater transmitter power, improved receiver sensitivity, new low-loss components and light-weight rapid-scan antennas are necessary. Source stability for coherent operation must be greatly improved. For implementation of the recognition/classification techniques, target characteristics, clutter effects and atmospheric effects are among the phenomenology that must be thoroughly documented.

Boost phase plume detection

Calculations have been performed to determine the feasibility of detecting missile plumes during the boost phase of the vehicle [22]. In the altitude regime of 30-100 km, it has been shown that, for a solid propellant system, molecular species, e. g. H_2O and H Cl, emit to permit radiometric detection from aircraft or satellites. Airborne radiometric observations are required to confirm predictions. The necessary passive technology is developing but must be extended to wavelengths as short as ~350 μm. Independent analysis of the bus stage indicate that spectral line opacity is sufficiently high to be detectable in occultation against the earth's radiation.

Conclusions

From the studies which have been performed, it can be concluded that the NMMW region offers a compromise for good resolution under adverse propagation conditions. Most systems, which have been investigated, profit from the narrow antenna beams available at NMM wavelengths, but are limited by atmospheric conditions. In some cases, the range limitations imposed by the atmosphere serve as an advantage for convert operation.

In order to utilize the NMMW spectral region properly, considerable technology must be developed. High-power sources, low loss components, precision antennas, sensitive receivers and stable local oscillators are priority devices to allow systems operations to be performed at NMM wavelengths. For many systems, highly coherent transmitters are required. This necessitates development of phase-locking and injection-locking technology for high-power sources. A driving force in extending military operation to NMM wavelengths is the prospect of small-size systems where space and antenna apertures are limited. Low cost, which is not a current characteristic of NMMW components, is expected to be an ultimate achievable goal.

One cannot expect to achieve everything that a system demands by employing NMM waves, and those working in the field are not doing this. Phenomenology in the form of atmospheric, terrain/clutter, target, and materials characteristics must be thoroughly developed for comparison with operation at other wavelengths. Thus far, studies have estimated certain characteristics and projected reasonable operational parameters for devices. From the considerations that have been made, optimum operation can be expected from hybrid IR/NMMW systems which will utilize the best of both spectral regions.

This work has been sponsored in part by the Harry Diamond Laboratories through the Army Research Office Contract No. DAAG29-77-C-0026.

References

1. 1974 Millimeter Wavelength Technical Conference, NELC/TD 308 Naval Electronics Laboratory Center, San Diego, CA 26-28, March 1974;

Proceedings of the DARPA/Tri-Service Millimeter Wave Conferences (8), Defense Advanced Research Projects Agency, Arlington, VA 22209

2. J. J. Gallagher, M. D. Blue, R. G. Shackelford, "Applications of Extreme Infrared to Missile Systems", Final Report on Basic Agreement DAHCO4-72-A0001, Task Order 76-8, Battelle Columbus Laboratories, January, 1976;

L. D. Strom, "Applications for Millimeter Radars", System Planning Corporation, Report No. 108, Contract No. DNA001-73-C-0098, ARPA Order No. 2353, December, 1973 AD529566;

"Low Probability of Intercept Multifunctional Tactical Sensors", Final Report, Contract F33615-76-C-1227, Raytheon Company, January, 1978;

Paul W. Kruse and Vitalij Garber, "Technology for Battlefield Target Recognition in Inclement Weather", Proceedings of the 23rd Annual IRIS Conference, 1976;

K. L. Koester, "Millimeter Wave Propagation", Norden Div. of United Technologies, Report 4392R005, 1972 (U);

A. M. Peterson, et al, "Low Angle Radar Tracking", Stanford Research Inst. Tech. Rept. JSR 74-7(U) February 1976, pages 53-57, 97-98;

J. J. Gallagher et al, "Applications of Submillimeter Wave Gigawatt Sources", Ga. Inst. of Technology, Engr. Experiment Station, Report GT/EES Project A-1717, DARPA Order 2840, 1975 (U);

R. LeLevier, "Applications of High Power Microwave/Millimeter Wave Technology" (U), R. and D Associates, Strategic Technology Final Report RDA-TR-4600-018, July 1975 (Report Secret);

Victor W. Richard, "Millimeter Wave Radar Applications to Weapons Systems", Ballistic Research Laboratories Memorandum Report No. 2631, June 1976 (U);

K. Evans, J. Dooley, R. Haraway, and H. Green, "Applications of Millimeter Wave Technology to Antiarmor Weapons Systems", Technical Report C-77-6, 22 February, 1977, U. S. Army Missile Research and Development Command, Redstone Arsenal, Alabama 35809

3. R. K. Parker, T. F. Godlove, and V. L. Granatstein, "Applications of High Power Microwave Sources - A Panel Study" (U), Vol. 1. NRL Memorandum Report 3339 (1976) (Report Secret);

"Interim Report on the Ad Hoc Study Group on the Military Applications of Millimeter Waves" Nato Document AC/243-D/332, AC/243(Panel III)D/115, June 1974 (U);

S. M. Kulpa and E. A. Brown, "DARCOM/DARPA Near-Millimeter Wave Technology Base Study", Harry Diamond Laboratories (1979);

4. S. M. Kulpa and E. A. Brown, "Propagation and Target/Background Characteristics", Volume 1 of Near-Millimeter Wave Technology Base Study, Harry Diamond Laboratories, October, 1979;

5. J. Preissner, "The Influence of the Atmosphere on Passive Radiometric Measurements", AGARD Conference Proceedings No. 245, Millimeter and Submillimeter Wave Propagation and Circuits, edited by E. Spitz, pp. 48-1 to 48-14, 4-8 September, 1978;

6. N. E. Feldman and S. J. Dudzinsky, Jr., "A New Approach to Millimeter-Wave Communications", R-1936-RC, April, 1977;

7. J. J. Gallagher, G. Loefer, J. L. Edwards, and J. P. Burns, "Microwave Instrumentation Applied to Aerosols and Smokes", Final Report, Contract No. DAA15-76-C-0087, 7 January 1979;

R. W. McMillan, R. Rogers, R. Platt, D. Guillory, J. J. Gallagher, and D. E. Snider, "Millimeter Wave Propagation through Battlefield Dust", Final Report, ASL-CR-79-0026-1, Contract DAAG29-77-C-0026, June, 1979;

J. J. Gallagher, R. C. Rogers, O. A. Simpson and J. H. Rainwater, "Millimeter Wave Propagation Through Smokes", Final Report, Contract No. DAAA11-77-C-0099, October, 1979;

8. G. D. Lukes, "Penetrability of Haze, Fog, Clouds and Precipitation by Radiant Energy Over the Spectral Range 0.1 Micron to 10 Centimeters", Naval Warfare Analysis Group of the Center for Naval Analysis, Study No. 61, under Contract N00014-68-A-0091, November, 1968;

9. H. J. Aufm Kampe, "Visibility and Liquid Water Content in Clouds in the Free Atmosphere", Journ. of Met 1, 54 (1970)

10. D. Deirmendjian, "Scattering and Polarization Properties of Water Clouds and Hazes in the Visible and Infrared", Applied Optics 3 , #2, 187-196, February 1964.

11. V. W. Richards and J. E. Kammerer, "Rain Backscatter Measurements and Theory at Millimeter Wavelengths", Ballistic Research Laboratories, Report No. 1838, October 1975.

12. See Reference 5.

13. N. A. Armand, A. O. Izyumov, and A. V. Sokolov, "Fluctuations of Submillimeter Waves in a Turbulent Atmosphere", Radio Engineering and Electronics Physics 16, 8, 1259 (August, 1971)

14. D. E. Snider, J. C. Wiltse, and R. W. McMillan, "The Effects of Atmospheric Turbulence and Adverse Weather on Near-Ground 94 and 140 GHz Systems", Workshop on Millimeter and Submillimeter Atmospheric Systems, Redstone Arsenal, Alabama, March, 1979.

15. J. H. Van Vleck and V. F. Weisskopf, Rev. Mod. Phys. 17, 227 (1945)

16. E. P. Gross, "Shape of Collision-broadened Spectral Line", Phys. Rev. 97, 394 (1955)

17. N. E. Gaut and E. C. Reifenstein, III, Environmental Research and Technology Report No. 13, NASA Contract NAS8-26275, Waltham, MA

18. R. A. Bohlander, et al, "Excess Absorption by Water Vapor and Comparison with Theoretical Dimer Absorption", D. T. Llewellyn-Jones, "Laboratory Measurements of Absorption by Water Vapor in the Frequency Range 100-1000 GHz", and H. A. Gebbie, "Observations of Anomalous Absorption in the Atmosphere", Proceedings of the Workshop on Atmospheric Water Vapor, Vail, Colorado, 11-13 September, 1979 (Institute for Atmospheric Optics and Remote Sension, Hampton, Virginia 23666)

19. A. H. Green and F. King, "Preliminary Millimeter Beamrider Feasibility Assessment", Internal Technical Note RE-77-3, Advanced Sensors Directorate, U. S. Army Missile Research, Development and Engineering Laboratory, U. S. Army Missile Command, Redstone Arsenal, 1 October, 1976.

20. D. G. Bauerle, R. A. McGee, J. E. Knox and H. B. Wallace, "140 GHz Beamrider Feasibility Experiment", Interim Memorandum Report No. 538, Ballistic Research Laboratories, January, 1977.

21. R. G. Shackelford and J. J. Gallagher, "Millimeter Wave Beamrider System", Advanced Sensors Directorate, U. S. Army Missile Research and Development Command, Technical Report TE-CR-77-7, August, 1977.

22. J. J. Gallagher, P. B. Reinhart, R. W. McMillan and J. H. Rainwater, "The Investigation of the Feasibility of Airborne Detection of Submillimeter Missile Plume Radiation", Final Report, Contract No. DASG60-78-C-0031 (February 22, 1979).